<u>GEORGIA DOT RESEARCH PROJECT 14-33</u>
FINAL REPORT

Assessment of High Early Strength Limestone Blended Cement for Next Generation Transportation Structures

OFFICE OF RESEARCH
15 Kennedy Drive
Forest Park, Georgia 30297-2534

Final Report

Assessment of High Early Strength Limestone Blended Cement for Next Generation Transportation Structures

By

Ahmad Shalan, Lawrence F. Kahn, Kimberly Kurtis, and Elizabeth Nadelman
Georgia Institute of Technology

Contract with

National Center for Transportation Systems Productivity and Management and
Georgia Department of Transportation

In cooperation with

U.S. Department of Transportation, Federal Highway Administration

December 2016

1. Report No.: FHWA-GA-17-1433	2. Government Accession No.:	3. Recipient's Catalog No.:
4. Title and Subtitle: Assessment of High Early Strength Limestone Blended Cement for Next Generation Transportation Structures	5. Report Date: December 2016	
	6. Performing Organization Code:	
7. Author(s): Ahmad Shalan, L. Kahn, K. E. Kurtis, and E. Nadelman	8. Performing Organ. Report No.:	
9. Performing Organization School of Civil & Environmental Engineering Georgia Institute of Technology Atlanta, GA 30332-0355	10. Work Unit No.:	
	11. Contract or Grant No.: GDOT Project No. 0013114 (RP 14-33, UTC sub-project)	
12. Sponsoring Agency Georgia Dept of Transportation 15 Kennedy Dr., Forest Park, GA & National Center for Transportation Systems Productivity and Management	13. Type of Report and Period Covered: Final; May 2014 – December 2016	
	14. Sponsoring Agency Code:	

15. Supplementary Notes:
   Prepared in cooperation with the U.S. Department of Transportation, Federal Highway Administration and USDOT Office of Research and Technology

16. Abstract:

   This research on Type IL cements for high early strength concretes demonstrated that Type IL cements satisfying AASHTO M 240 specifications may be used in place of Type I/II cements which satisfy AASHTO M 85 specifications for construction of transportation structures such as precast prestressed bridge girders. Type I/II and Type IL cements from five producers were investigated. The cements and both mortars and concretes made with these cements were studied to determine material characteristics; material properties including setting time, strength development, shrinkage, creep, permeability; and structural properties for use in precast prestressed bridge girders. Tests of 30-ft long beams made with 8,000 psi design strength concrete using Type IL and with Type I/II cements and ½-in. diameter 270 ksi prestressing strands showed that the prestress losses were about 5% less than those predicted using the refined method of AASHTO LRFD (7th edition, 2016). Further, strand transfer length was less than one-half of that specified, and the development length was less than 45% of the length specified in AASHTO LRFD (7th edition, 2016). Flexural strength of the beams was greater than that calculated based on actual concrete strength and prestressing forces.

   The fineness of portland-limestone cements leads to higher shrinkage than Type I/II cements for water-cementitious materials ratios (w/cm) greater than 0.45, but for the high early strength concretes with w/cm less than 0.4, no significant difference in shrinkage was noted.

17. Key Words: Cement, Limestone, Structural Concrete, Prestressed Concrete	18. Distribution Statement:		
19. Security Classification (of this report): Unclassified	20. Security Classification (of this page): Unclassified	21. Number of Pages: 85	22. Price:

EXECUTIVE SUMMARY

This research on Type IL cements for high early strength concretes demonstrated that Type IL cements satisfying AASHTO M 240 specifications may be used in place of Type I/II cements, which satisfy AASHTO M 85 specifications for construction of transportation structures such as precast prestressed bridge girders. Type I/II and Type IL cements from five producers were investigated. The cements and both mortars and concretes made with these cements were studied to determine material characteristics; material properties including setting time, strength development, shrinkage, creep, and permeability; and structural properties for use in precast prestressed bridge girders. Tests of 30-ft long beams made with 8,000 psi design strength concrete using Type IL and Type I/II cements and reinforced with ½-in. diameter 270 ksi prestressing strands showed that the prestress losses were about 5% less than those predicted using the refined method of AASHTO LRFD (7th edition, 2016). Further, strand transfer length was less than one-half of that specified, and the development length was less than 45% of the length specified in AASHTO LRFD (7th edition, 2016). Flexural strength of the beams was greater than that calculated based on actual concrete strength and prestressing forces.

When produced with greater fineness, use of portland-limestone cements leads to higher shrinkage than Type I/II cements for water-cementitious materials ratios (*w/cm*) greater than 0.45. But for the high early strength concretes with *w/cm* less than 0.4, no significant difference in shrinkage was noted. Supplementary cementitious materials including Class C fly ash, Class F fly ash, and ground granulated blast furnace slag may be used with Type IL cements just as they are used with Type I/II cements. Permeability of the high early strength concrete measured by the Resistance of Concrete to Chloride Ion Penetration Test (RCPT) [AASHTO T 277, 2011] and by surface resistivity [AASHTO TP 95, 2011] resulted in a "low" value (RCPT about equal to or less than 2000 coulombs).

ACKNOWLEDGMENTS

Table of Contents

List of Tables

List of Figures

Chapter 1 – Introduction

1.1 Purpose and Objectives

The purpose of this research was to examine the performance of limestone blended cement for use in high early strength concrete for construction of concrete bridge structures including prestressed concrete girders. The main objectives were related to examining the effects of increasing limestone addition rate up to 15% by mass replacement of portland cement for high early strength concrete construction. Objectives included (1) assessment of key material properties such as setting time, strength development, shrinkage, creep, and permeability, and (2) determination of whether prestressed concrete beams made with Type IL cements would perform the same as beams made with Type I/II cements meeting Georgia DOT class AAA [GDOT Specification Section 500 – Concrete Structures].

The structural performance of Type IL concrete was assessed by testing four full-scale prestressed beams. The specific objectives of the tests were to determine prestressing strand bond strength, development length and transfer length; to determine the flexural strength; to quantify prestressing losses, and to compare these behaviors with beams made using Type I/II cement and with AASHTO LRFD bridge design standards.

The final objective was to provide guidance on the use of Type IL cements with up to 15% interground limestone for precast concrete elements intended for transportation structures and possible changes to state and federal specifications.

1.2 Research Motivation

Both AASHTO and ASTM have recently approved a significant change to their specification for blended cements. In 2012, both associations – in AASHTO M 240 [2012] and in ASTM C595 [2013] specifications – adopted specifications allowing an increase in the allowable mass of ground limestone ($CaCO_3$) in some portland cement compositions to approximately 15% by mass; this is an increase over a prior recent change allowing ground limestone additions, but limiting them to less than 5% by mass [AASHTO M 85, 2008 and ASTM C150, 2012]. This new class of "limestone blended cements" are anticipated to have significantly different behavior than currently available binders due to the higher limestone fraction [Lothenbach et al., 2008 and Hawkins et al., 2003]. Currently, higher percentages of limestone powder are allowed in Canada and Europe, where specifications allow up to 15% and 35% by mass.

A key impetus for the change in cement composition is growing concerns about the environmental implications of cement manufacture and increasing demand for sustainable next generation infrastructure development [Bentz et al, 2012]. The partial replacement of cement clinker with ground limestone is associated with contributions to sustainability due to significant reductions in energy consumption during cement manufacture and reductions in emissions of carbon dioxide, other gases, and particulates during production. Thus, with increasing energy costs and increasing interest in reducing the environmental impacts associated with the use of cement and concrete, US cement standards have changed, allowing for 'greener' cement compositions. The ultimate potential contributions of these new cements to sustainability will depend, however, upon their ability to perform as well as or better than traditional cements, considering cracking resistance, mechanical properties and durability, and allowing for extended concrete service lives.

However, because ground limestone is largely chemically inert, portland cements containing limestone are generally ground more finely to compensate for the lower reactivity of the blend. For example, the fineness of limestone blended cement is typically ~5-40% finer than a comparable ASTM C150 Type I/II cement suitable for general use [Bonavetti et al., 2000]. For certain applications, even greater finenesses are found. For example, a limestone blended cement designed as an alternative to ASTM C150 Type III high early strength cements, fineness may be ~40-70% greater than traditional cements. As a result, the rate of cement reaction, time to set, and early age shrinkage, among other properties, are affected [Bentz et al., 2012]. While faster early hydration and shorter setting times may be favorable for precast applications, increased shrinkage is potentially problematic. Cracking may result from excessive shrinkage, compromising durability. Shrinkage and creep can also result in loss of prestress, which can reduce structural capacity in prestressed sections.

However, most of this research examining the influence of limestone in blended cements has been performed at relatively low limestone usage rates (i.e., 5% by mass or less) and in cements with moderately increased fineness. There is less understanding of the effects of greater limestone replacement rates, and virtually no published research considering the very fine (i.e., ~600 m^2/kg) blended cements targeted for applications – such as precast bridge elements – requiring high early strength.

Because relatively little research has been conducted on the dimensional stability and the durability of such cements, their use in structural concrete, including prestressed concrete applications where high-early strength and cracking resistance are paramount should be considered. With their recent adoption in ASTM and AASHTO standards, with the potential economic and environmental benefits of their use relative to ordinary cements, the proliferation of limestone blended cements is expected within the next few

years. Therefore, behavior of the higher limestone blended cements, and in particular those ground more finely to achieve high early strength, must be assessed independently in a comprehensive investigation, to ensure that their performance can meet state and federal specifications.

Concrete containing limestone blended cements, particularly when combined with supplementary cementitious materials (SCMs), can likely be produced more economically than with traditional cements. If such binder compositions are shown to result in greater dimensional stability (i.e., crack resistance when restrained) and improved durability, additional long-term savings can be realized through reduced maintenance and extended service lives. However, these assessments are needed, as only limited data are available in the literature and, unfortunately, very little third-party data address finely ground, high early strength limestone cements specifically. Increasing energy costs, carbon taxes, and limited availability of traditional cements are all additional factors which could contribute to future cost savings associated with the use of limestone blended cements in place of traditional cements.

1.3 Scope

The scope of this study was based on findings found in the concurrent research project "Assessment of Limestone Blended Cements for Transportation Applications," funded by the Georgia Department of Transportation (GDOT), Research Project No. 13-09. Findings from the concurrent GDOT research permitted the more limited materials investigation conducted in this study. The concurrent study investigated eleven cements, portland Type I/II and Type IL cements with up to 15% interground limestone from five producers. All of these cements, and two Type IL in particular, were investigated in this research; those two represented the breadth of behaviors found previously. Use of those two permitted concentrated investigation for application to class AAA concrete for high early strength structural applications. The one Type IL cement which was available from a single producer of both Type I/II and IL cements and with the same grind was chosen for beam construction so that an exact comparison of structural performance of Type I/II and Type IL concretes could be made.

Material studies included investigation of curing at standard, room temperature conditions (73°F) and curing at elevated temperature (140°F) to simulate steam curing conditions used for some precast concrete bridge girders.

Even with the limitations discussed and as detailed in Chapter 3, hundreds of material samples were made and were tested for material characterization, fresh concrete properties, and long-term permeability and mechanical properties.

Chapter 2 – Background

2.1 Introduction

Portland limestone cements, or PLCs, originated in Europe in the 1960s [Tennis et al., 2011 and Livesey, 1991], but have only recently been considered for use in the United States and Canada. As early as 1960, Spanish standards permitted the use of cements containing up to 10% limestone by weight (later revised to 35%), while French standards adopted in 1979 allowed up to 35% limestone by weight [Tennis et al., 2011]. By incorporating a finely ground "filler" material in place of a fraction of the traditional portland cement, the total amount of clinker produced – and therefore the total amount of energy consumed – could be reduced.

As in Europe, the gradual introduction of portland limestone cements in the North American market has come about as a result of growing concerns over the environmental impacts of cement production – in terms of both its energy consumption and the CO_2 emissions generated during manufacture. In 2004, the American Society for Testing and Materials (ASTM) approved the inclusion of up to 5% limestone (LS) in all cements specified under its ASTM C150 standard [2004], and in 2012 approved the inclusion of up to 15% limestone under its ASTM C595 designation [2012]. Similar allowances were approved by the American Association of State Highway and Transportation Officials (AASHTO) in AASHTO M85 [2012].

2.2 Hydration

When it was first incorporated into portland cements, finely divided limestone was believed to act as a chemically inert filler, occupying space that would otherwise be filled by either unhydrated cement grains or capillary porosity. However, recent research has shown that limestone "fillers" play several important roles in the early hydration of portland cement pastes, not only physically but chemically, as well.

Previous studies of chemical effects of limestone on portland cement hydration indicated that in the presence of calcium carbonate ($C\bar{C}$), the hydration reactions are slightly altered. While the C_3S, C_2S, and the initial C_3A reactions all proceed in the same manner as in ordinary portland cements, thermodynamic models [Matschei et al., 2007 and Lothenbach et al. 2008] have suggested that the secondary conversion of ettringite into monosulfate will not occur when sufficient calcium carbonate is present. The stabilization of the ettringite and the additional formation of carboaluminate phases is consequently believed to increase the volume of hydration products relative to ordinary cement pastes, leading to an overall reduction in the capillary porosity of the hydrated cement paste; however, such effects have not been experimentally demonstrated.

The fineness of limestone powders and their dispersion throughout the cement paste also result in physical effects that may alter the kinetics of cement hydration. These physical effects include filler effects, nucleation effects, and dilution effects, each of which is illustrated in Figure 2.1.
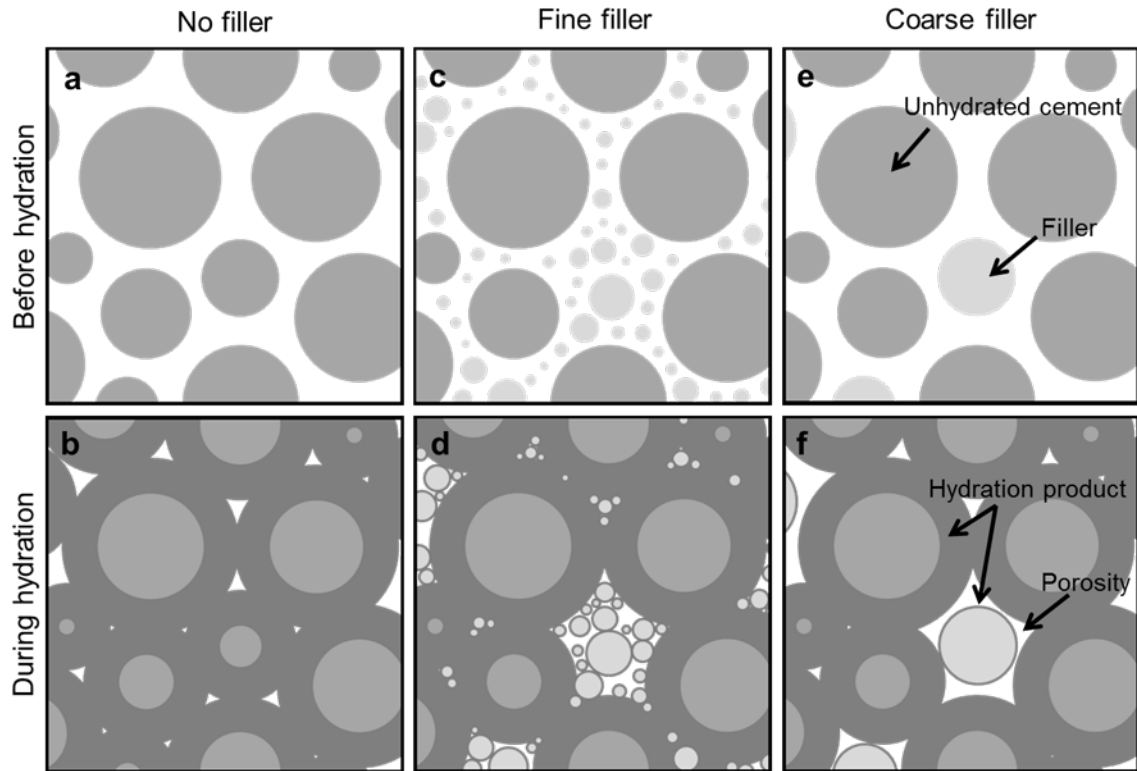
Figure 2.1 Schematic representation of the effect of a 10% volumetric filler replacement on cement hydration. Filler effects dominate in the presence of fine fillers (c & d), while dilution effects dominate in the presence of coarse fillers (e & f) [from Nadelman, 2016].

The filler effect, shown in Figure 2.1c and d, refers to the wider dispersion of the cement grains and the improved packing of the solid phases that result from the change in particle size distribution [Isaia et al. 2003]. Nucleation effects (Figure 2.1d and f) are caused by the increase in solid surface area due to the fine limestone addition; they are especially pronounced for limestone additions [Kadri et al., 2010 and Oey et al., 2013]. Accompanying – and possibly counteracting – the filler and nucleation effects is the dilution effect (Figure 2.1e and f), which results from the substitution of the reactive cement clinker by a less reactive limestone filler. Whereas portland cement clinker typically has a specific gravity of about 3.15, limestone has a specific gravity of only about 2.7 [Balonis and Glasser, 2009], which increases the volume of solids in the system when the limestone is used as a partial clinker replacement on an equivalent-mass basis.

Replacing 10% of the clinker by mass, for example, will increase the solid volume of the system by approximately 1.6%. The increase in the solid volume creates a slightly denser packing of solid particles in the initial cement paste matrix, resulting in a secondary filler effect that is independent of particle size.

2.3 Findings from Georgia DOT Sponsored Research

The Georgia DOT sponsored research project 13-09, "Assessment of Limestone Blended Cements for Transportation Applications," which was conducted concurrently with this study. Nadelman [2016] reported some of the findings from that concurrent research, and some of those findings are presented below as background.

2.3.1 Material characterization

Eleven cements from five sources in the southeastern United States (Figure 2.2) were considered for this companion GDOT study. Sources were randomly assigned designations A-E to preserve anonymity. One ASTM C150 Type I/II ordinary portland cement (LS ≤ 5%) and at least one companion ASTM C595 Type IL portland limestone cement (LS ≤ 15%) produced from the same clinker were provided from each source. One Type IL cement was received from each source A-D, while two Type IL cements of identical composition and varying fineness (designated CG for more coarsely ground and FG for more finely ground) were received from source E. In the following analysis and discussion, Type I/II cements are indicated by their single letter source name (e.g., cement A), while Type IL cements are indicated by their single letter source name plus the letter "L" (e.g., cement AL).

Figure 2.2. Geographic sources for cements investigated. The dashed line between Calera, AL and Roberta, GA indicates that the Argos clinker was produced in Calera, AL and finished in Roberta, GA.

The chemical compositions of each cement were obtained by oxide analysis [ASTM C114, 2013] and quantitative x-ray diffraction (XRD) [ASTM C1365 2011]. In terms of chemical composition, all five portland cements conform to ASTM C150 Type I/II specifications [2016], but contain a range of C_3S, C_2S, C_3A, and C_4AF contents. Based on the XRD analyses, the cements from source E contain the highest amount of C_3S (contributing to early strength and microstructural development), while the cements from sources A and B have more C_2S (contributing to later age strength and microstructural development).

The limestone content of each cement was additionally measured by thermogravimetric analysis (TGA) under nitrogen environment, using a Hitachi EXSTAR TG/DTA 7300. $CaCO_3$ contents were calculated based on the mass loss between approximately 600°C and 750°C, wherein $CaCO_3$ thermally decomposes into CaO and $CO_2\uparrow$. All five Type IL cements contained limestone contents within the 5-15% permissible range of ASTM C595 as shown in Figure 2.3. Type I/II and Type IL cements for each source originate from clinkers having approximately the same specific gravity; therefore, they likely originate from the same clinker.
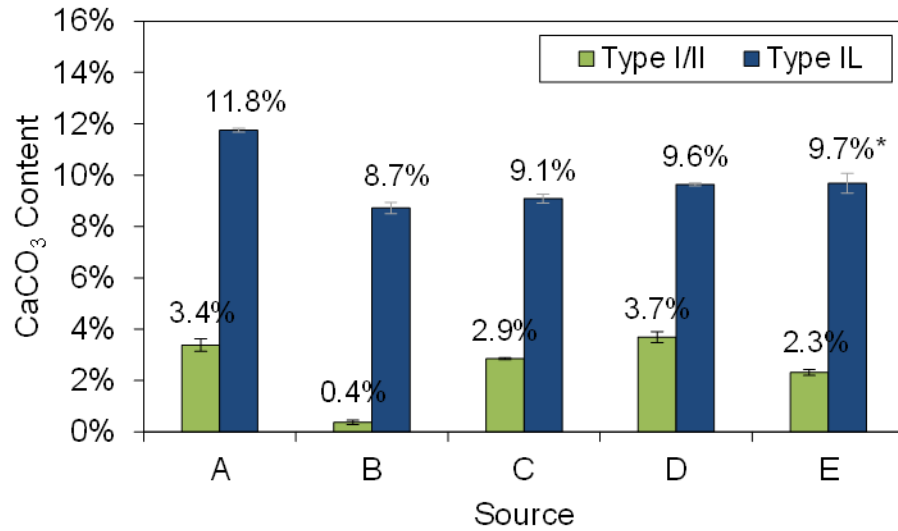
Figure 2.3 CaCO$_3$ contents of cements A-E determined by TGA. Error bars indicate one standard deviation.

With the exception of Blaine fineness, which was obtained according to ASTM C204 [2011], all of the particle size parameters for the eleven cements were obtained by laser diffraction in ethanol using a Malvern Mastersizer 3000E. Based on the particle size distributions, it can be observed that there are generally two categories of Type IL cements considered in this study: those with significantly finer particle size distributions than their Type I/II companion cements (cements AL, DL, and EL, both CG and FG), and those with broader but similar particle size distributions to their Type I/II companion cements (cements BL and CL).

Hydration studies found that limestone fillers increased the rate and amount of crystalline calcium hydroxide (CH) precipitation at early ages for finely ground Type IL cements (e.g., cement AL) and to dilute the overall amount of CH (and by extension, other hydration products) existing in the paste at later ages. The former effect can be attributed to increased heterogeneous nucleation of hydration products on the surfaces of the limestone, which results in an acceleration of the hydration reaction as observed by isothermal calorimetry. The latter effect can be attributed to the dilution of the cement by a less reactive filler, and additionally results in the lower cumulative heats of hydration observed by isothermal calorimetry for the Type IL cements. Finely ground Type IL cements promote the nucleation of hydration products (especially CH) and accelerate hydration within the first few hours of mixing, which, in turn, lead to finer microstructures at the earliest ages of hydration. Coarsely ground Type IL cements were

also shown to experience nucleation effects at very early ages due to their increased specific surface area, but these effects were largely overcome by the more dominant dilution effects and slower clinker hydration rates within only a few hours of hydration.

Research further demonstrated that limestone is not simply an inert filler, and, in addition to altering hydration and microstructural development through physical means, it also has a significant impact on chemical evolution. In particular, it was demonstrated that even small substitutions of limestone (< 5% by mass) can result in the formation of carbonate AFm (monosulfoaluminate hydrate, monosulfate) phases and the indirect stabilization of ettringite.

2.3.2 Chemical and autogenous shrinkage

Cement pastes with water-to binder ratio (*w/b*) of 0.40 were prepared from each of the eleven commercially produced cements. Chemical shrinkage was measured by dilatometry according to ASTM C1608 [2012]. Autogenous shrinkage was measured for each cement paste in accordance with ASTM C1698 [2009]. Chemical shrinkage results showed behavior consistent with heat of hydration, in which the more finely ground Type IL cements from sources A, D, and E exhibited greater amounts of chemical shrinkage relative to their Type I/II counterparts, while the more coarsely ground Type IL cements from sources B and C exhibited lesser amounts of chemical shrinkage relative to their Type I/II counterparts. Autogenous shrinkage results also indicate that the more finely ground Type IL cements (from sources A, D, and E) tend to experience greater degrees of autogenous shrinkage when compared to Type I/II cements of the same clinker composition. Linear strains were increased by as much as 200 μm/m by 56 days for cement pastes AL, DL and EL, suggesting that the more refined microstructures and more rapid rates of hydration for the finely ground Type IL cement pastes result in greater contractions than would be expected for conventional Type I/II cement pastes at the same age.

For the cements from sources B and C, the autogenous deformation of the more coarsely ground Type IL cement pastes was lower in magnitude than the autogenous deformation of the Type I/II companion pastes through the first 7 days of hydration.

Cement pastes made from finely ground Type IL cements exhibited the greatest relative increases in chemical and autogenous shrinkage, which were attributed to their increased rates of hydration and microstructural development as a result of filler and nucleation effects. On the other hand, cement pastes made from the more coarsely ground Type IL cements initially exhibited a relative decrease in early-age shrinkage as a consequence of dilution-dominated hydration, but were found to show potential increases in shrinkage beyond 7 days of hydration due to contributions from more slowly reacting clinker phases such as C_4AF. At a w/b of 0.40, chemical shrinkage accounted for

approximately 97% of the early-age shrinkage experienced by the eleven cement pastes considered.

2.3.3 Interactions with supplementary cementitious materials (SCMs)

Previous studies have shown that when SCMs are combined with portland limestone cements, even greater improvements in durability will result from further refinements in porosity and increases in strength and impermeability [De Weerdt et al., 2011a; De Weerdt et al., 2011b; Vance et al. 2013; and Menendez et al. 2003]. In this GDOT study, thirty-three cement paste mixtures were prepared from the eleven cements and three SCMs (Class F fly ash, Class C fly ash, and ground granulated blast furnace slag) at a water-to-cementitious materials ratio (*w/cm*) of 0.40. Measured compressive strengths for the 12 SCM-blended class AA concrete mixtures are shown in Figure 2.4. With respect to the neat concrete mixtures, the data show that the more finely ground Type IL cement from source A produces concrete with early-age (< 28 days) strengths comparatively higher than those made from the companion Type I/II cement, consistent with the more rapid rates of hydration and microstructural development. As the dilution effects begin to supersede the early-age nucleation effects, the compressive strengths of the A and AL mixtures become more similar to one another, and are statistically indistinguishable by 90 days. The more similar particle size distributions for the two cements led to more similar rates of hydration and microstructural development at all ages.

Mixtures containing SCMs were generally found to have lower strengths than the control mixtures at 1 day of age as a consequence of the dilution of the cement by the more slowly reacting SCMs, but over time, the secondary pozzolanic and latent hydraulic reactions produced concretes with equivalent or higher compressive strengths relative to the control mixtures by 90 days. By 28 days, although some of the Type I/II-SCM blends still exhibited lower compressive strengths compared to the Type I/II control, all 6 mixtures containing Type IL cements had statistically equivalent or greater compressive strengths, indicating that blends of Type IL cements with SCMs can be used to overcome dilution effects and achieve functionally equivalent strengths by 28 days [Barcelo et al., 2013].
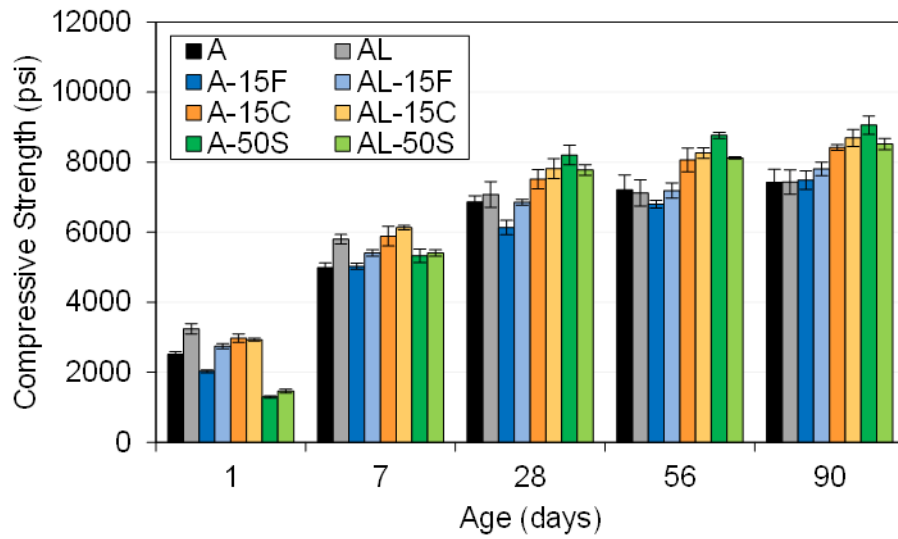
(a)
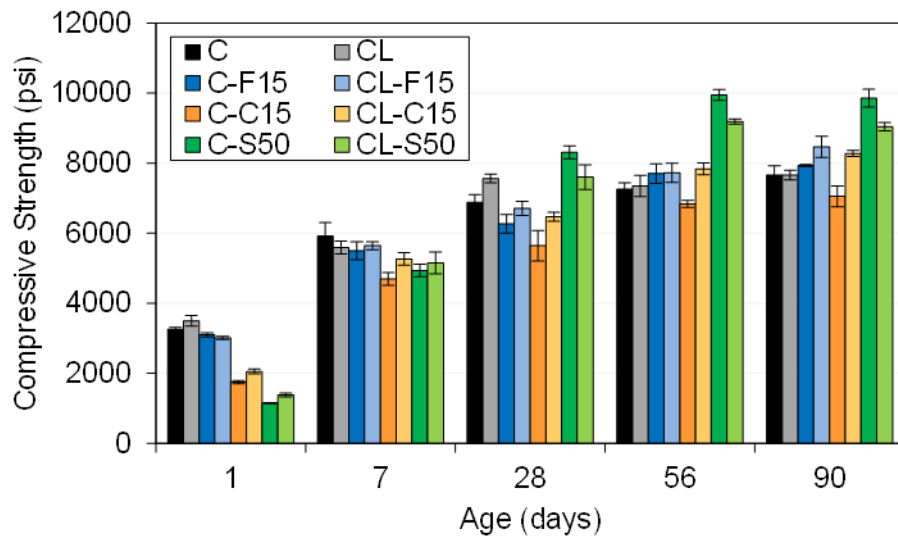
(b)

Figure 2.4. Compressive strength development for concrete mixtures from sources (a) A and (b) C, each containing SCMs at w/cm = 0.445.

Blends with 15% Class F fly ash developed strengths at rates most similar to the control mixtures, and by 90 days hydration were found for both sources to increase compressive strength by up to 10% (800 psi) relative to the neat concrete mixtures. Blends of Class F fly ash with Type IL cements, on average, exhibited strengths 500 psi greater at 90 days than the blends of Class F fly ash with Type I/II cements, suggesting a

supplementary strengthening effect caused by interactions between the limestone fillers and the fly ash.

The blends containing 50% slag exhibited the greatest strength gains over the first 90 days of hydration, reaching more than 9000 psi for mixes from both sources. At a 50% slag replacement level, no synergetic increases in compressive strength were observed for the Type IL mixes; instead, the Type IL-slag mixes were found to be, on average, 700 psi weaker by 90 days compared to the Type I/II-slag blends.

Blends of Type IL cements with SCMs can be suitably used as replacements for Type I/II cements in construction applications. Despite the dilution of the cement by the limestone filler, equivalent or more refined porosities – resulting in equivalent or higher strengths – can be achieved when Type IL cements are partially substituted with 15% fly ash or 50% slag, by mass. While blends of Type IL cements with 15% Class C fly ash were able to achieve higher strengths at 56 days when compared to the Type I/II control mixtures, the increases in strength came at the expense of increased chemical and autogenous shrinkage at early-ages, which could increase cracking in structural applications. By contrast, blends of Type IL cements with 15% Class F fly ash were found to provide the best balance in properties, slightly increasing compressive strength by 56 days, while still reducing early-age chemical and autogenous shrinkage.

2.3.4 Permeability

Twenty-three concrete mixtures containing various combinations of PLCs and SCMs were assessed using the ASTM C1202/AASHTO T277 rapid chloride permeability test (RCPT) and the AASHTO TP95 [Tennis et al., 2011] surface resistivity (SR) test. Eleven were neat cement mixtures using each of the commercially-produced cements, and twelve were SCM-blended mixtures using the cements from sources A and C. All 23 mixtures were prepared to meet Georgia Department of Transportation (GDOT) Section 500 specifications for class AA concrete [GDOT Specification 500, 2015], a class of concrete specified for use in bridge superstructures which may therefore require low permeability to aggressive environments such as sea water and sulfate exposure [Holland et al., 2012]. To investigate the "worst-case" permeability for this class of concrete, the maximum permitted water-to-cementitious-materials ratio (w/cm = 0.445) and the minimum permitted cementitious materials content (635 lb/yd3, or 375 kg/m3) were selected for each mix. SCMs, when used, were substituted for cement at the maximum GDOT allowed replacement levels: 15% for Class F and Class C fly ashes, and 50% for slag.

The results of the RCP test again indicate that there is little difference between the electrical properties for the Type I/II and Type IL concretes without SCMs as shown in Figure 2.5. In blends with SCMs, the Type IL cements showed slightly greater

reductions in total charge passed when blended with 15% Class F fly ash or 50% slag, but the magnitude of the reduction was, in general, not statistically significant. Mixed results were obtained for the concretes containing 15% Class C fly ash, where there was essentially no difference at 56 days between mixes A and AL, but a more than 30% reduction in charge passed for mix CL versus C as shown in Figure 2.6.
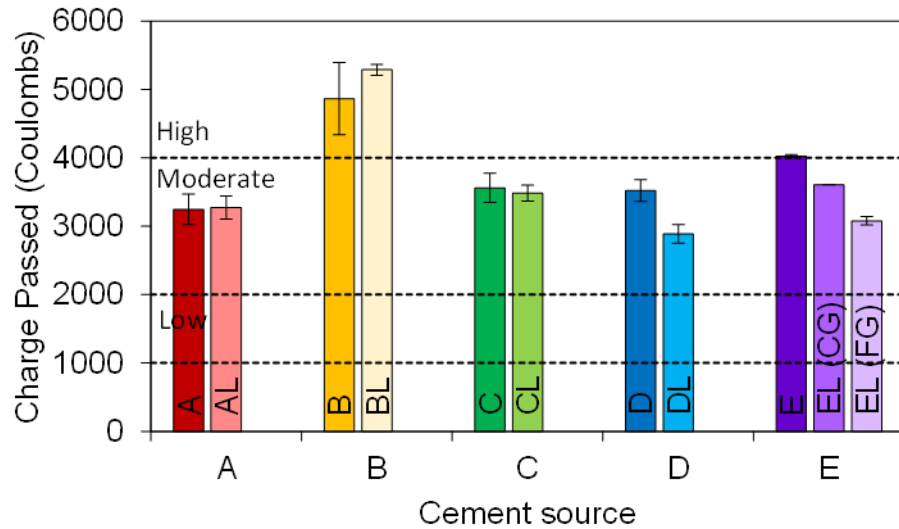
Figure 2.5. Total charge passed by RCPT for concretes A-E, after 56 days of hydration. Error bars indicate the range of values obtained for each mixture.
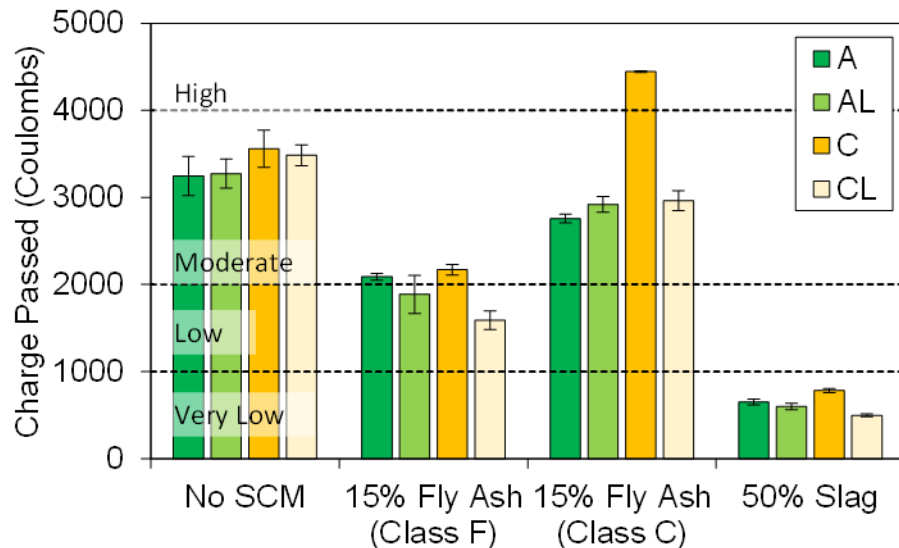
Figure 2.6. Total charge passed by RCPT for concretes containing SCMs, after 56 days of hydration. Error bars indicate the range of values obtained for each mixture.

Comparing the 56 day SR and RCPT results to one another, the two tests had a nearly perfect inverse relationship to one another.

The results of the study indicated that, in general, limestone substitutions to portland cement had a small effect on the long-term microstructural development of neat concrete mixtures and ultimately yield concretes with similar permeabilities to traditional portland cement concretes. When combined with SCMs, the limestone appears to accelerate the pozzolanic and latent hydraulic reactions of the SCMs, producing concrete with generally more refined microstructures and reduced permeabilities as a result.

Chapter 3 – Experimental Program

The experimental program involved three main phases. First, materials were obtained from various sources that differed in location and cement characteristics such as fineness and limestone source. Second, two curing conditions were used to resemble room temperature conditions and high temperature used in precast concrete construction (discussed in more details in following sections). Third, a group of testing methods were conducted to compare the characteristics and performance of Type I/II and Type IL cements.

3.1 Materials

Materials were received from 5 cement plants. Each plant provided Type I/II cement and Type IL cement. Table 3.1 gives limestone characteristics.

Table 3.1. Cements used for this research

Producer	Limestone characteristics
(A)	Limestone (dolomite) LS replacement rate (14-15%)
(B)	Softer limestone
(C)	Limestone (marl)
(D)	Softer limestone
(E)	Two limestones (fine, coarse)

Concrete samples were produced using all materials. In a separate study done by Georgia Tech for GDOT, class AA concrete was made using cement from all above producers.

After examining the properties and performance of all cements, it was found that cement fineness had significant effects on the performance of concrete. This study (RP 14-33) focused on high early strength concrete where class AAA concrete was produced and studied. Cement producer "A" had finer Type IL cement while producer "C" had Type IL cement with a fineness more similar to that of the Type I/II cement. Based on that, cement from producers "A" and "C" were selected for this study.

After contacting ready-mixed concrete producers in Atlanta, and taking into account the availability of Type IL cement in Georgia market for precast construction, Producer

"C" was selected for the construction of the four prestressed beams at Tindal Corporation.

3.2 Curing Conditions

Two curing conditions were used: Room temperature (73°F, according to ASTM 192) and high temperature (140°F). High temperature curing is commonly used in precast concrete construction to accelerate strength development. Figure 3.1 shows the saturated lime-water baths used for curing samples at room temperature. Figure 3.2 shows the curing box used for high temperature curing.

Figure 3.1. Saturated lime-water baths for curing at room temperature

Figure 3.2. Intellicure temperature controlled curing box for high temperature curing

3.3 Characterization of Type I/II and Type IL Cements

The first step to identify key differences between Type I/II and Type IL cement was to compare their physical and chemical properties in terms of particle size, hydration kinetics, and phases present in each type of cement. The methods used were particle size analysis, isothermal calorimetry, quantitative X-ray diffraction analysis (QXRD), and Vicat time of setting [ASTM C191, 2013].

3.3.1 Particle size analysis

Particle size analysis was conducted on all cements to investigate the effect of fineness of cement and ground limestone on concrete performance. The instrumentation used was Malvern Mastersizer 3000 (Figure 3.3), which is a laser diffraction particle size analyzer. Ethanol was used as a solvent instead of water to prevent cement hydration while running the measurements.

Figure 3.3. Malvern Mastersizer 3000

3.3.2 Isothermal calorimetry

Isothermal calorimetry was conducted for all cements at room temperature (73°F) and at 140°F to compare the hydration kinetics of limestone cements to Type I/II cements. The instrument used was TAM Air Isothermal Calorimeter (Figure 3.4). Sand was used for the reference ampoules at high temperature after it showed better

performance than empty ampoules since sand is an inert material with approximately the same heat capacity as the sample in the reference.

Figure 3.4. TAM Air Isothermal Calorimeter

3.3.3 Quantitative X-ray diffraction analysis (QXRD)

QXRD was conducted to compare the phases present in samples of the cements received. Samples were sent to Heidelberg Technology Center in Atlanta where QXRD was performed at its facilities.

3.3.4 Time of setting

Vicat time of setting [ASTM C191] was conducted for all cements at room temperature and at 140°F (which is the precast curing temperature) to compare the initial and final setting times of limestone cements to Type I/II cements which are important parameters for constructability. The instrument used was ToniSET (Figure 3.5), which is an automatic Vicat needle instrument at Heidelberg Technology Center.

Figure 3.5. ToniSET automatic Vicat instrument

3.4 Concrete Mix Design

Several concrete producers in the State of Georgia were consulted for concrete mix designs for high strength concrete. The design strength was 8 ksi at 28 days which is a typical value used for prestressed concrete in bridge girder applications, and it is greater than the 5000 psi minimum required strength. All the requirements of GDOT Specification 500 and Specification 865 for class AAA concrete and prestressed girder concrete needed to be met as well. Therefore, trial batches were produced and high range water reducer was needed to achieve the required slump and was obtained from Sika (Sika Viscocrete 2100).

The coarse aggregate size was number 67, and the aggregate was obtained from Vulcan Materials in Lithia Springs, GA. The fine aggregate was natural sand obtained from Lambert Materials in Atlanta, GA.

Class AAA concrete mixes were produced using cement from producers A and C according to the mix design in Table 3.2. Batch quantities for class AA and class A mixes are shown in Table 3.2 for comparison. The class AAA used a high range water reducer at a rate of 5 oz. per 100 lbs. of cement. Concrete batching was performed at room temperature (73-75°F).

Table 3.2. Concrete mix design

Material	Class AAA (lb/yd3)	Class AA (lb/yd^3)	Class A (lb/yd^3)
Cement	800	635	611
Water	256	282	299
Coarse Aggregates	1890	1890	1890
Fine Aggregates	1096	1253	1229
w/c (water-cement ratio)	0.320	0.445	0.489
Mininum Required 28-day strength (psi)	5000*	3500	3000

*Note that the design strength for the beams was 8000 psi which is typical for highway girders

3.5 Fresh Properties of Class AAA Concretes

Fresh concrete properties of class AAA concretes were compared between Type I/II and Type IL cements. These properties included time of setting, slump, unit weight, and air content.

Concrete was prepared in the Structures and Materials Laboratory at Georgia Institute of Technology following the specifications of ASTM C192. Slump [ASTM C143], unit weight [ASTM C138], and air content [ASTM C231] were measured and compared for Type I/II and Type IL cements immediately after each concrete mix was made. Prior to the production of concrete, the researcher was certified as a Concrete Field Testing Technician Grade I by the American Concrete Institute.

3.6 Concrete Mechanical Properties

Mechanical properties of concretes made with Type I/II and Type IL cements were measured. Those included compressive strength, elastic modulus, and split-cylinder tensile strength. Figure 3.6 shows concrete mixing, placing, and measurement of fresh properties.

3.6.1 Compressive strength development (ASTM C39)

Compressive strength of concrete cylinders was measured for class AAA concrete at 1 day, 3 days, 7 days, 28 days, 56 days, and 90 days. For each test, three 4-in. x 8-in. cylinders were used. An Instron 800,000 lb. testing machine was used with automated load-rate control.

| (i) Concrete mixing | (ii) Concrete filled into molds |

| (iii) Slump test | (iv) Unit weight test | (v) Air content test |

Figure 3.6. Concrete mixing, placing, and measurement of fresh properties

3.6.2 Elastic modulus (ASTM C469)

Elastic modulus was measured using 6-in. x12-in. cylinder samples at 28 days of age (Figure 3.7). Samples were loaded to 40% of their compressive strength (which was measured immediately before the test). Instron compression machine was used with automated load-rate control. The deflections were measured using mounted analog dial gages placed on the side of the concrete cylinder. The deflection data were video recorded simultaneously with the load data. The videos were then analyzed and load-displacement data were extracted. For each test, three 6-in. x 12-in. cylinders were used. Each cylinder was tested three times.

Figure 3.7. Gages for measuring deflections for the Elastic modulus test

3.6.3 Splitting tensile strength (ASTM C496)

Splitting tensile strength was measured for concrete samples at 28 days of age
(Figure 3.8). An Instron compression machine was used with automated load control.
For each test, three 4-in. x 8-in. cylinders were used.

Figure 3.8. Splitting tensile test sample

3.7 Shrinkage and Creep Behavior

3.7.1 Drying shrinkage

Drying shrinkage prisms (3 in. x 3 in. x 10 in.) were cured in lime-saturated water for 28 days (ASTM C157), and then drying initiated at standard room temperature and humidity. Measurements were then taken at 4 days, 7, days, 14 days, 4 weeks, 8 weeks, 16 weeks, and 32 weeks using a length comparator (Figure 3.9).

A second group of samples was only cured for 7 days (Alabama DOT Standard Specifications for highway construction Section 501), and then drying was measured at the same drying times given above. Curing for only 7 days was used since the shorter curing time more accurately reflects field curing conditions for structural concrete.

Figure 3.9. Drying shrinkage sample with length comparator

3.7.2 Creep (ASTM C512)

Creep samples were made using 4-in. diameter cylinders, 15-in. long molds as shown in Figure 3.10. Steel circular plates were placed at the two ends of the molds and were permanently attached to the cylinders. Two cylinders were stacked in each loading frame as shown in Figure 3.11. The circular end plates for each cylinder had pins or holes at their centers. This was used to reduce the eccentricity between the stacked cylinders.

The samples were cured identically to compression test samples for 3 days. They were then loaded to 40% of their compressive strength capacity. Loading at 3 days of age was selected to simulate the maturity of the concrete at which time prestressing is

applied; that is when prestressing strands are cut. A detachable mechanical multi-length strain gage (Figure 3.12) was used to measure the creep strain while a load cell was used to measure the load applied.

Figure 3.10. Mold used for creep specimens with embedded nuts for DEMEC measurements

Figure 3.11. Creep frames

Figure 3.12. Detachable mechanical strain gage (DEMEC).

3.8 Prestressed Concrete Beam Design

This study also compared the performance of Type I/II and Type IL cements in prestressed concrete girder applications. Prestressed beams were designed to measure prestress losses, strand transfer length, strand development length, and beam flexural strength.

The beams were designed according to the standards in AASHTO LRFD Bridge Design Specifications [2016]. The theoretical development length was calculated using AASHTO equation 5.11.4.2-1:

$$\ell_d \geq \kappa\left(f_{ps} - \frac{2}{3}f_{pe}\right)d_b \qquad \qquad Equation\ 3.1$$

where:

ℓ_d = development length

d_b = nominal strand dimeter (in.)

f_{ps} = average stress in prestressing steel at the time for which the nominal resistance of the member is required (ksi)

f_{pe} = effective stress in the prestressing steel after losses (ksi)

κ = 1.6 for pretensioned members with a depth greater 24 in.

Figure 3.13 shows the beam design. A depth of 25 in. was selected to satisfy the condition for using κ = 1.6, which more accurately represents prestressed concrete beams in bridge applications. Two strands were selected to allow averaging of data from each strand. One design consideration was to maximize the strain in the steel strands to test their bond with concrete; therefore, 270 ksi 7-wire low relaxation 0.5-in. diameter steel strands were selected. Another design consideration was to achieve flexural failure prior to shear failure. Therefore, a width of 10 in. was selected, which was also satisfied the spacing requirements between two steel strands, shear reinforcement, and concrete cover. The design of the concrete mix was identical to the concrete produced at the lab.
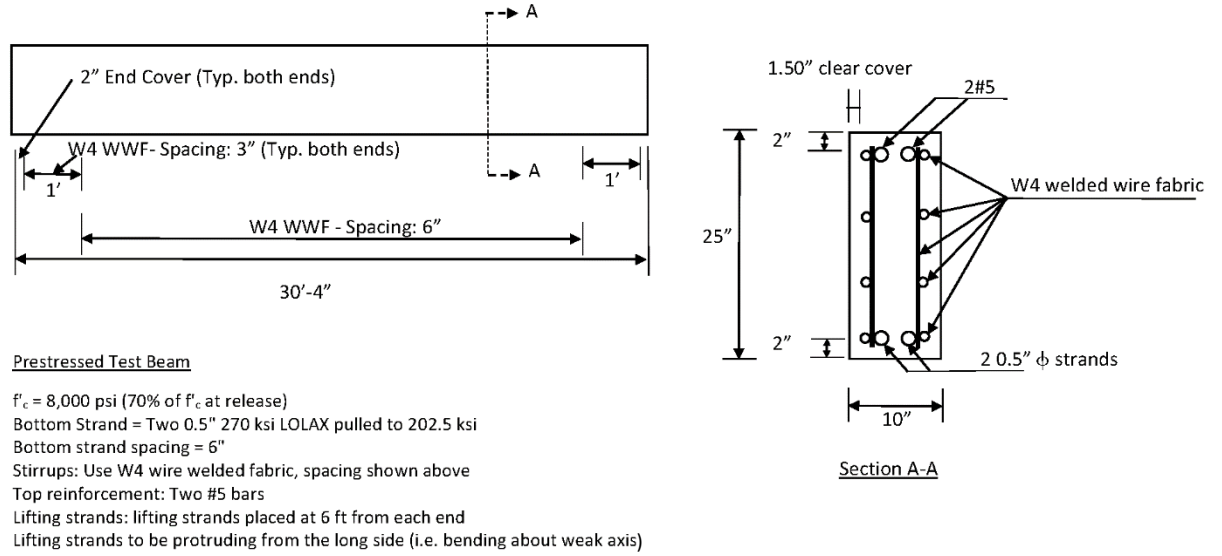
Figure 3.13. Prestressed beam design

3.9 Beam Construction

Four beams were produced at Tindall Corporation using class AAA concrete provided by Thomas Concrete with cement from plant C. Two beams were produced using Type I/II cement, while two other beams were produced using Type IL cement.

Figures 3.14 and 3.15 show formwork and prestressing anchorage, and concrete placement and finish, respectively. To minimize the cost of construction, the beams were cast on their side. Fresh concrete properties were tested on site as shown in Figure 3.16. Figure 3.17 shows samples of concrete cylinders that were also produced to measure their mechanical properties.

Figure 3.14. Formwork, welded-wire fabric, and prestressing
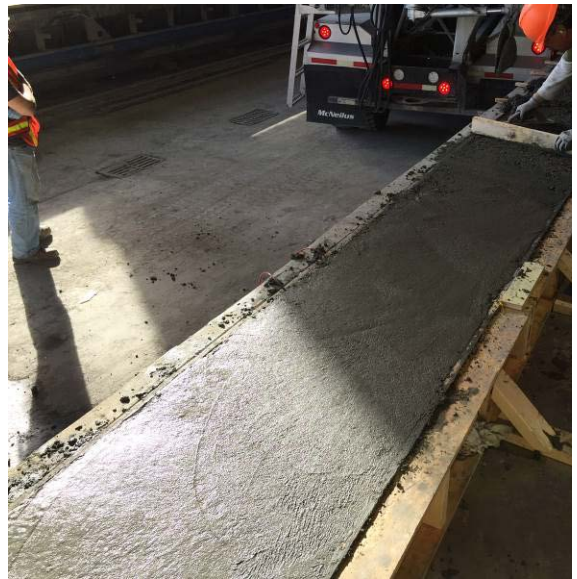
Figure 3.15. Placing concrete and finishing the surface for the beams

Figure 3.16 Measurement of fresh concrete properties

Figure 3.17. Preparation of concrete cylinders for mechanical testing

3.10 Structural Properties

To investigate the performance of limestone cement concretes in prestressed girders applications, four prestressed beams were produced at Tindal Corporation and trucked to the Structures and Materials Laboratory at Georgia Tech (Figure 3.18). Two beams were made with Type I/II cement concrete and the other two with Type IL cement concrete. Further, Mustafa test-blocks were constructed to investigate adequacy of bond between

prestressing strand and the two concrete types. The specimen design and test procedure followed the specifications given by Logan [1997].

The beams were used to measure prestress losses, strand transfer length, strand development length, and beam flexural strength. Three bending tests were performed on each beam: two for development length and the third for flexural capacity. The layout of each test was designed to prevent excessive damage in areas of the beam used for each subsequent test.

Figure 3.18. Delivery of the prestressed beams from Tindal Corporation to Georgia Tech.

3.10.1 Prestress losses

Prestress losses were measured using vibrating wire strain gages (Figure 3.19) that were placed at midspan of each beam at the level of the prestressing strands (Figure 3.20).   The strain measurements were taken beginning 3 hours after concrete placement and periodically until development length testing, between 128 and 152 days after stressing. The vibrating wire strain gages were model 4200 from Geokon. A portable handheld readout unit (Model GK-404) was used to read the strain and concrete temperature.

Figure 3.19. Vibrating wire strain gage and readout unit from Geokon

Figure 3.20. Installing vibrating-wire strain gages at midspan next to prestressing strands

3.10.2 Strand bond, Mustafa test for direct pull-out

Mustafa test for strand direct pull-out was performed to compare the non-prestressed bond strength of prestressing strands with concretes made with Type I/II and Type IL cement. The specimen design and test procedure followed the specifications given by Logan [1997].

One concrete block was made with Type I/II cement while the other was made with Type IL cement. Six strands were placed in each block. The strands were identical to the ones used for the beams (0.5-in. diameter steel strands 270 ksi 7-wire low relaxation strands). Each strand was 60 in. long. The blocks were 24 in. x 36 in. x 24 in. The strands were embedded to a depth of 19 in. under the top surface with PVC tubes placed at the top 2 in. to act as bond breakers. Figure 3.21 shows the design of the blocks for Mustafa

tests; Figure 3.22 shows the formwork; and Figure 3.23 shows concrete placement. Figure 3.24 shows the specimen and instrumentation used for the test. The load was measured using a load cell. The deflection was measured using a linear variable differential transformer (LVDT).
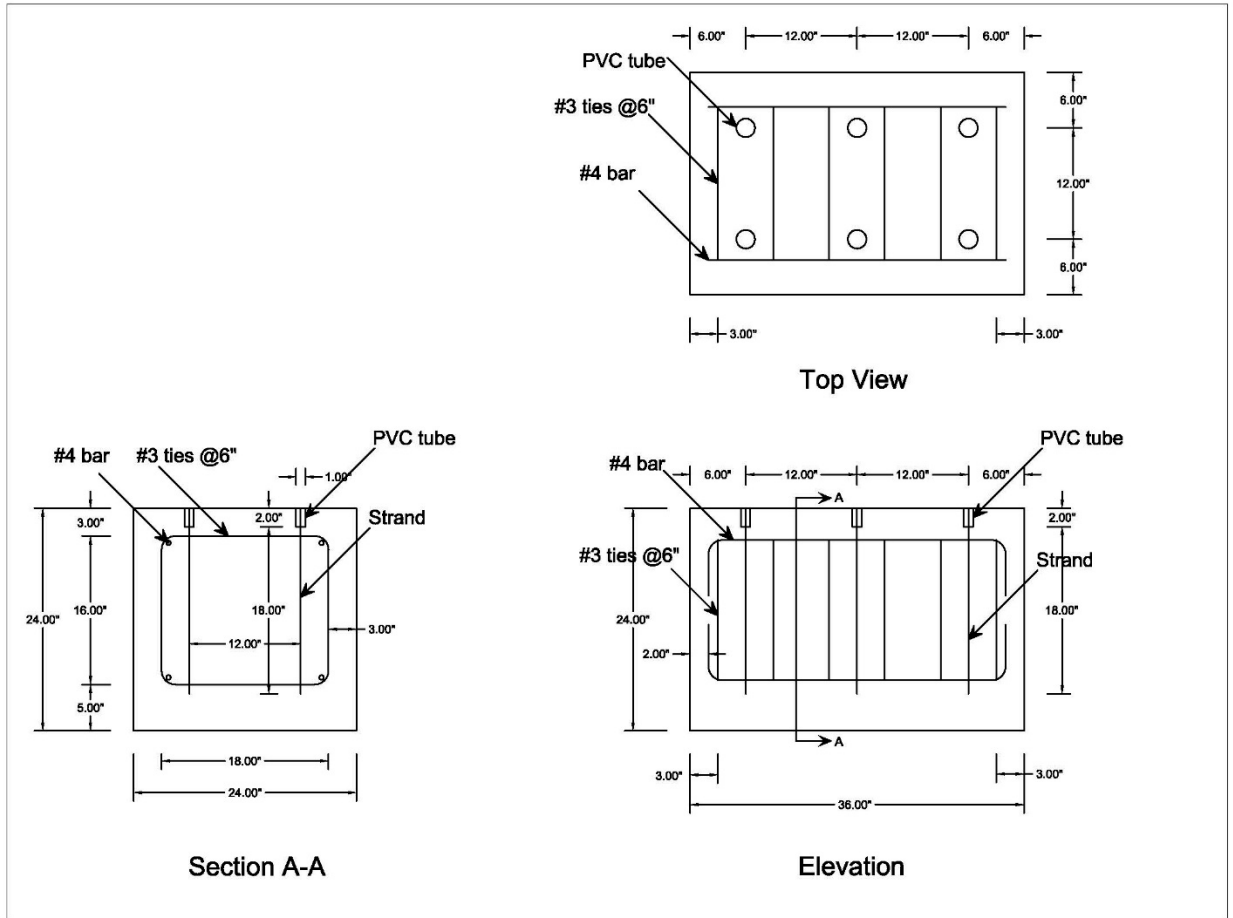
Figure 3.21. Design of concrete blocks for Mustafa test.

Figure 3.22. Formwork for Mustafa test specimens.

Figure 3.23. Placing concrete for Mustafa Pull-out test.
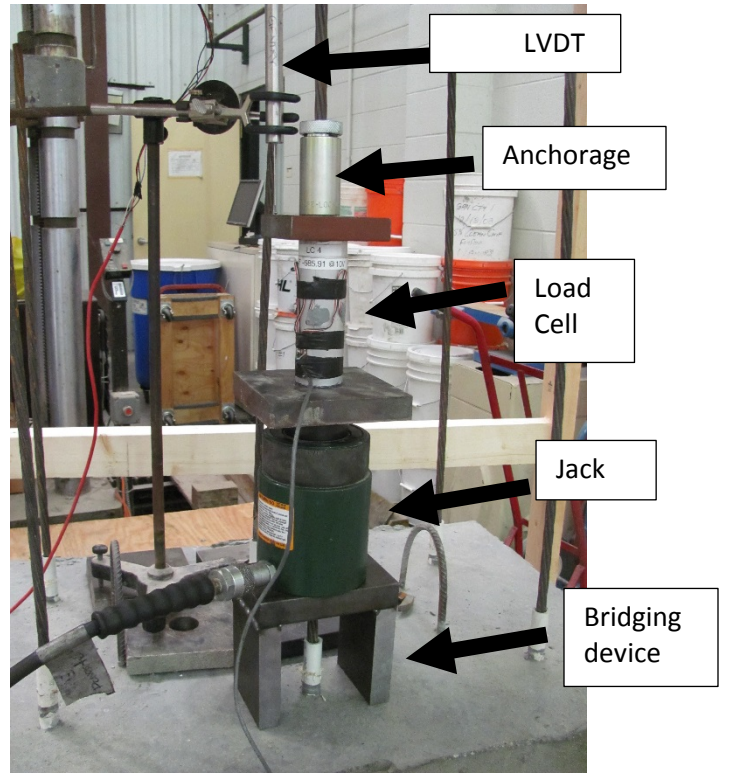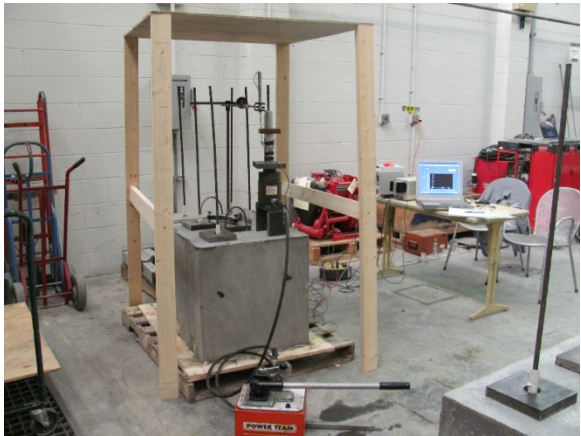
Figure 3.24. Specimen and instrumentation for the Mustafa test.

3.10.3 Transfer length

Transfer length was measured using a detachable mechanical strain gage (DEMEC). Readings were taken at the level of the prestressing strands. DEMEC points were steel T-nuts embedded in the side of each beam and were spaced 2–in. apart (Figure 3.25). The gage length used with the DEMEC gage was 8 in. The beams were cast on their side; so, the forms which held the DEMEC points in correct position were on the top of the sections being cast as shown in Figure 3.26.

Figure 3.25. Metal nuts for transfer length measurements.
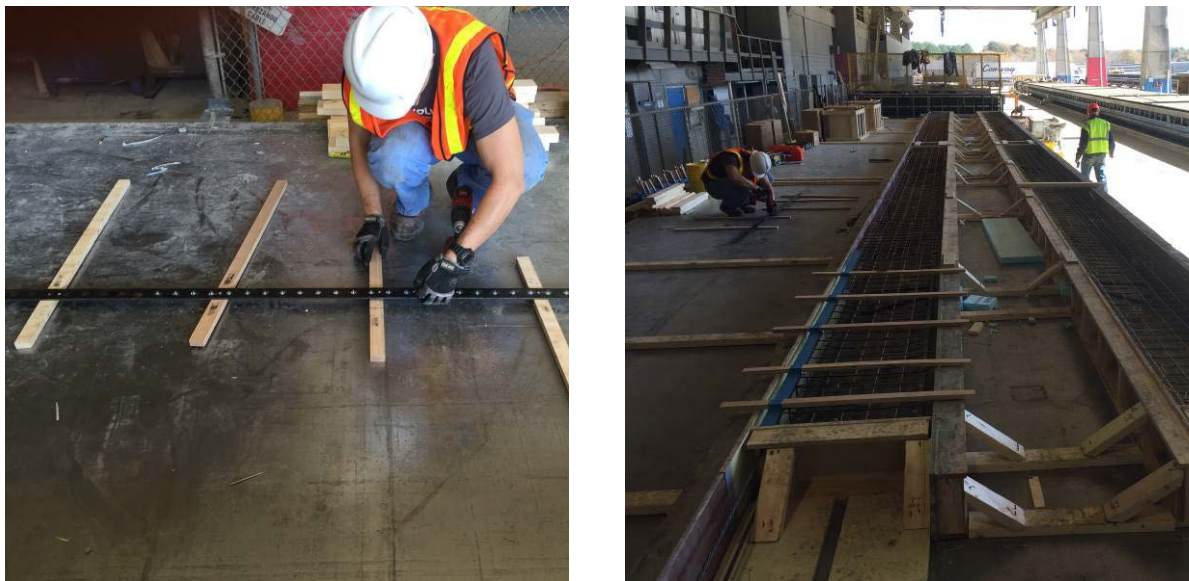
Figure 3.26. Placement of embedded nuts located in steel spacer bar for transfer length measurements.

3.10.4 Beam testing sequence

The following testing sequence was selected to run three bending tests on each beam while avoiding damaged areas from previous tests.

For the first test, the beam was supported over about two thirds of its length as shown in Figure 3.27. The center of one support was located 3-in. from the right end, while the second support location varied but was about 10 ft. from the left end. Load was applied at 90% of the AASHTO LRFD [2016] design development length from the right end for the first test.

For the second test, the beam was rotated so that the original right end was now at the left. The beam was again supported over about two-thirds of its length so that the undamaged, cantilevered zone from the first test was now subject to the load. The load was applied at 65% of the AASHTO design development length (equation 5.11.4.2-1) from the undamaged end.

For the third test, the beam was loaded at midspan, and the supports were moved inward leaving damaged areas from the previous two tests out of the tested segment.

The same sequence was applied again for the second beam but with 50% and 45% of the AASHTO design development length (equation 5.11.4.2-1) used instead of the 90% and 65%, respectively. To prevent a compression strut from forming, the shear span was kept greater than twice the depth of the beam. This is why the value of 45% of the AASHTO design development length (equation 5.11.4.2-1) was the minimum distance from the support to apply the load.

Table 3.3 summarizes the distance from the end to the load point and the span lengths for the development length tests while Table 3.4 gives the span lengths for the flexural strength tests.
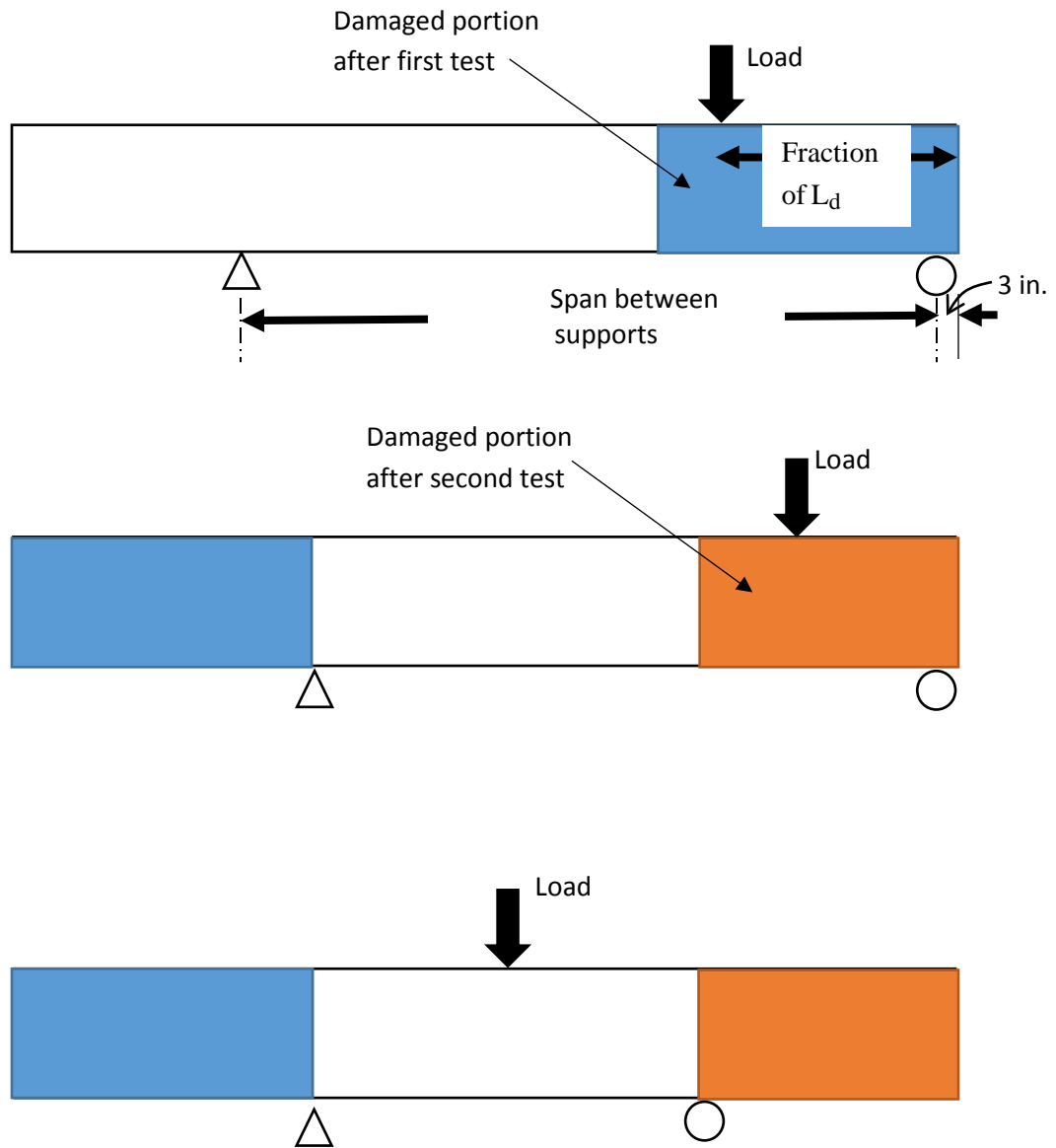
Figure 3.27. Sequence of beam tests

Table 3.3. Summary of testing protocol for development length tests

| Cement Type | Beam number | Distance between load application and beam end | | Span between supports (in.) |
		Relative to AASHTO development length (L_d)	Actual Value (in.)	
Type I/II	Beam 2	90%	111	261
	Beam 2	65%	80	209
	Beam 1	50%	62	264
	Beam 1	45%	56	264
Type IL	Beam 4	90%	111	261
	Beam 4	65%	80	209
	Beam 3	50%	62	264
	Beam 3	45%	56	264

Table 3.4. Spans used for flexural tests (load applied at center of the beam)

Cement Type	Beam number	Span between supports (in.)
Type I/II	Beam 2	135
Type IL	Beam 4	135
	Beam 3	135

3.10.5 Development length

As described in the testing layouts, loads were applied at various proportions from the theoretical [AASHTO LRFD, 2016] development length values. Gages were fixed to the end of the prestressing strands to measure any slip of the strands relative to the concrete surface as shown in Figure 3.28.
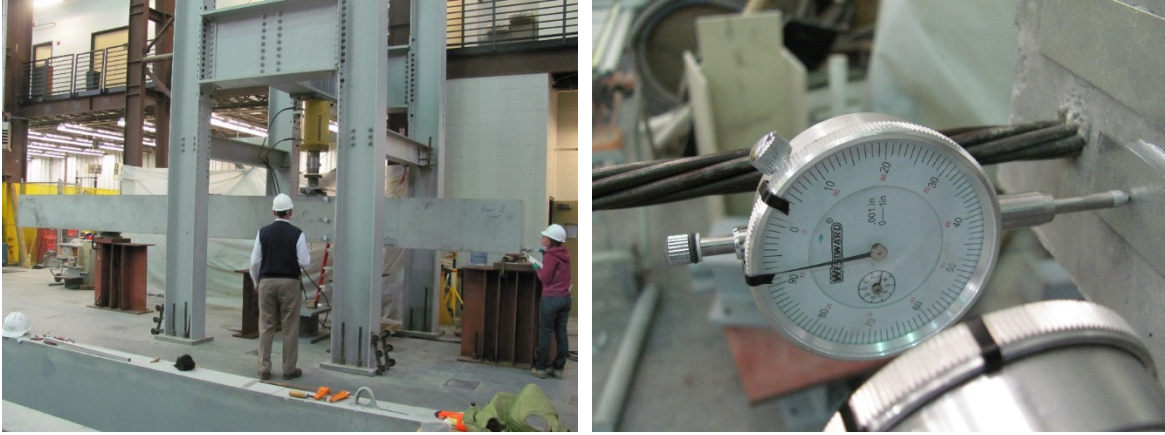
Figure 3.28. Development length test and gages used for measuring strand slip.

Dial gages were also placed at three levels of the beam under the point of load application to measure the strain 1-in. from the top of the beam, at mid-depth, and at the level of the strands as shown in Figure 3.29. The gage length used was 23 inches which was the depth (d_p distance) of the steel strands.
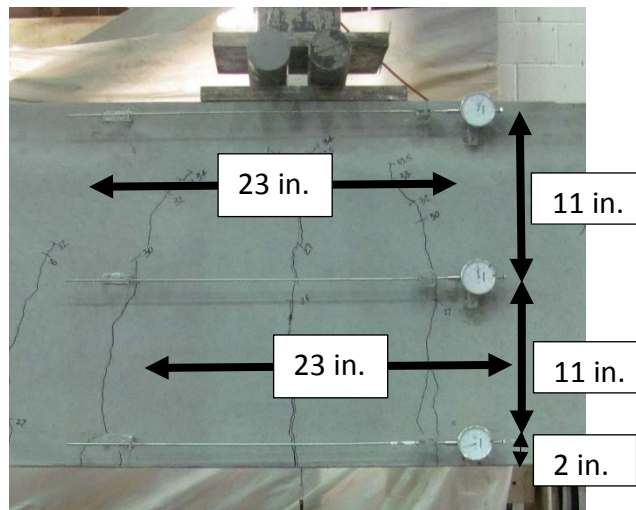
Figure 3.29. Dial gages placement for strain profile measurements under applied load

3.10.6 Flexural capacity

As described in the testing layouts, the load was applied at midspan during the third test of each beam to compare the flexural capacities of the beams. Strain profiles under the point of application of the load were also recorded. Figure 3.30 shows the overall test with the beam loaded at midspan.

Figure 3.30. Flexural strength test setup.

Chapter 4 – Results and Discussion

4.1 Characterization of Type I/II and Type IL Cements

4.1.1 Particle size analysis

Particle size analysis was performed on cements from all 5 plants and is shown in Table 4.1 and Figure 4.1. The results show that there were two groups of Type IL cements: Type IL with finer particle size than Type I/II and Type IL with similar particle size to Type I/II. It was observed that particle size was an important factor in predicting hydration, early-age shrinkage, and strength development rates. The Type IL cements from sources A, D, and E had finer particle size distributions compared to their Type I/II counterparts, but the Type IL cements from sources B and C were found to be more similar in gradation to the Type I/II cement. Coarse gradations for Type IL cements have been found in previous studies to correlate with slower rates of hydration, reduced early-age shrinkage, and slower rates of compressive strength development.

Table 4.1. Particle size summary for cements A-E.

Cement	Surface mean [μm]	Volume mean [μm]	D_{10} [μm]	D_{50} [μm]	D_{90} [μm]
A	6.28	14.1	2.77	10.0	30.2
AL	5.09	10.2	2.29	7.5	21.8
B	6.71	15.1	3.17	10.4	31.9
BL	5.83	14.3	2.41	10.1	32.1
C	6.53	15.1	3.03	10.1	34.1
CL	5.60	14.6	2.25	10.2	33.6
D	6.19	15.5	2.45	11.9	34.0
DL	5.66	12.9	2.37	9.5	28.6
E	7.07	16.8	3.15	11.8	36.2
EL (CG)	6.69	14.9	2.99	10.8	32.8
EL (FG)	5.72	11.8	2.54	8.9	25.4
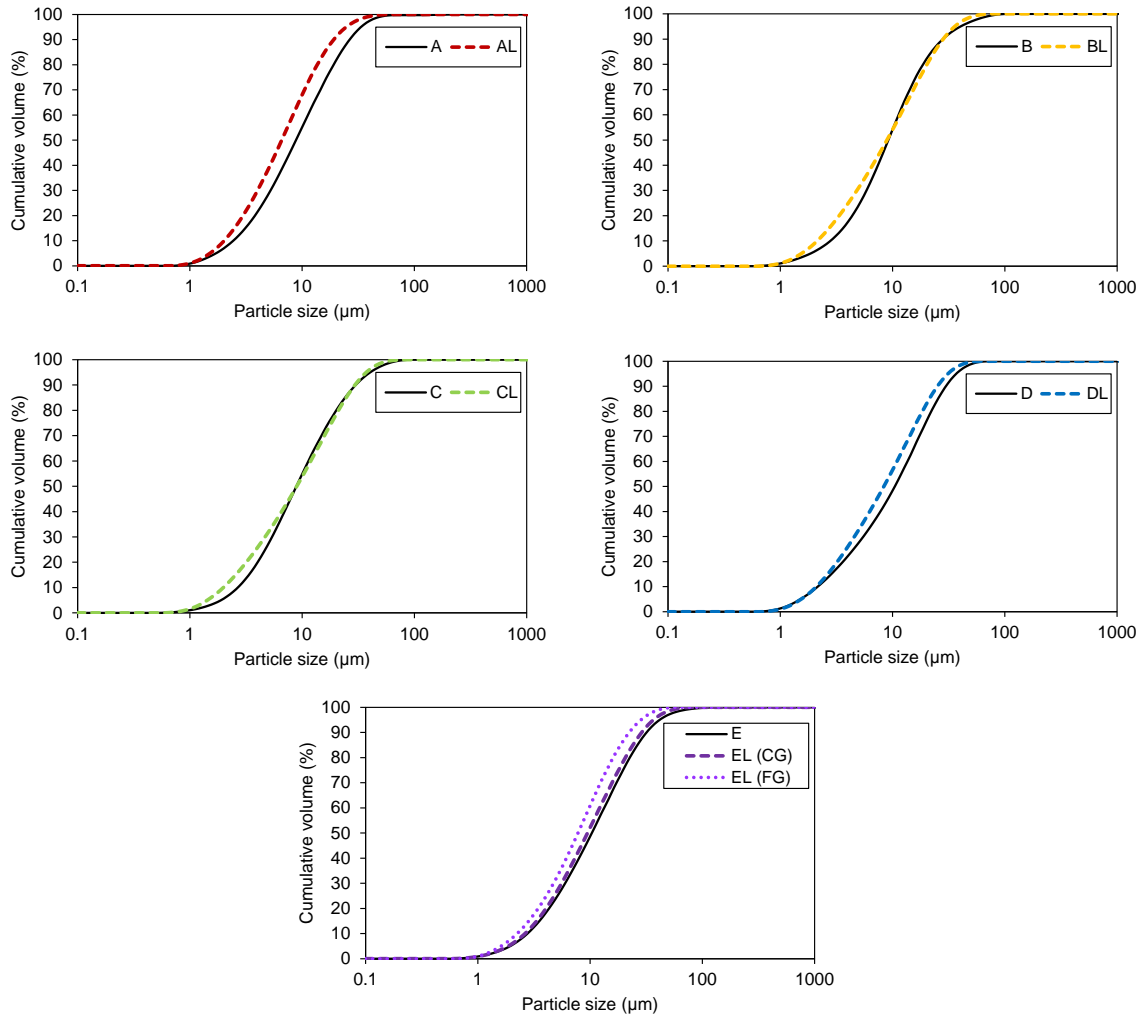
Figure 4.1.   Cumulative particle size distribution for cements A to E.

4.1.2 Isothermal calorimetry

Isothermal calorimetry was performed on cement pastes at 140°F for Cements A-E. Pastes were prepared at a w/c = 0.44 which is the maximum w/c specified for class AAA concrete in GDOT Section 500 [2013]. The results are shown in Figure 4.2.

Finer Type IL cements (AL, DL, ELC, and ELF) showed an accelerated hydration reaction compared to the companion Type I/II cement pastes, as indicated by the left shift of the heat release (measured as power) curves. The total cumulative heat converged with the companion Type I/II for these finer Type IL cements. On the other hand, the coarser Type IL cements (BL and CL) showed slower hydration and less cumulative heat than their companion Type I/II cements, indicating less total hydration.
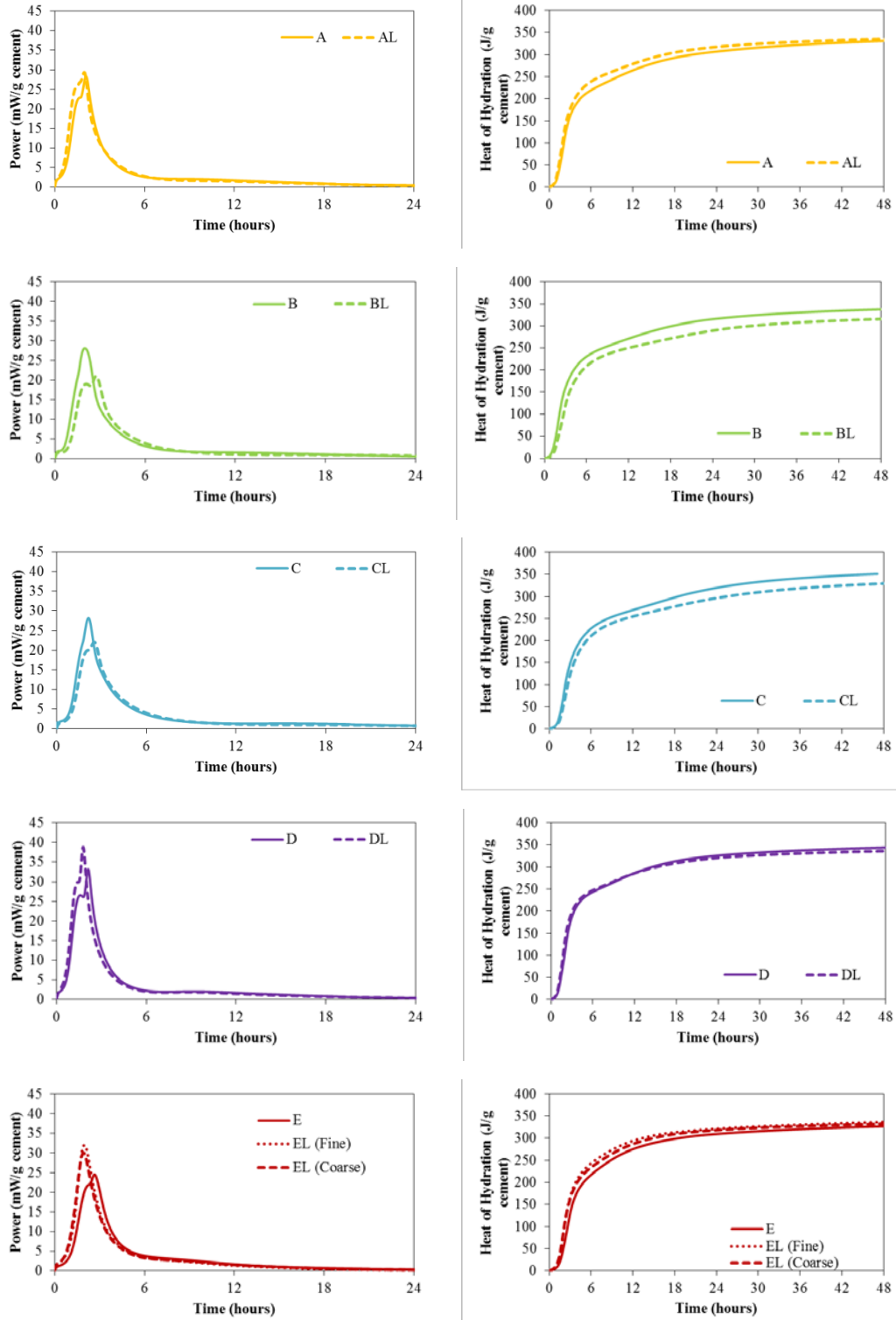
Figure 4.2. Calorimetry results (power and cumulative heat of hydration) for cements A to E at 140°F.

41

When compared to results of calorimetry performed at 73°F (conducted for the concurrent GDOT project), similar trends with cement fineness were observed. Figure 4.3 shows a comparison of the calorimetry results of cements from plants A and C at 73°F and 140°F.

For the finer Type IL cement (AL), Type IL cement produced higher cumulative heat than Type I/II cement at 73°F, while the cumulative heat converged at 140°F.

On the other hand, the coarser Type IL cement (CL) produced similar cumulative heat to Type I/II cement at 73°F, while Type IL cement produced lower cumulative heat than Type I/II cement at 140°F. These results suggest that early age strength development may be slightly delayed in precast concrete utilizing Type IL cements with similar fineness to Type I/II cements.
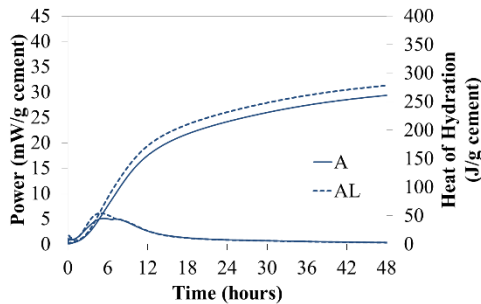
(a) Plant A at 73
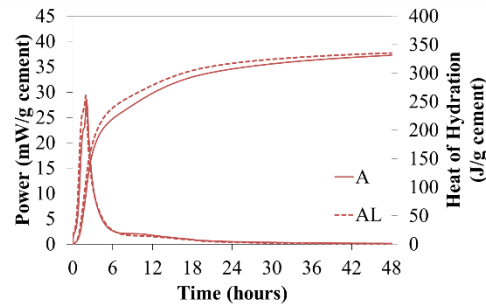
(b) Plant A at 140
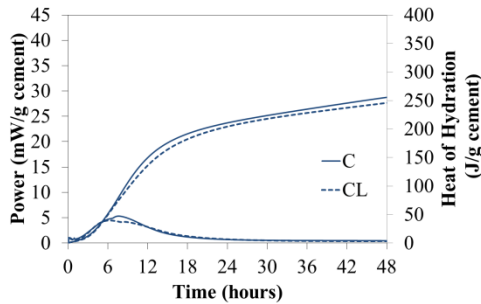
(c) Plant C at 73 °F
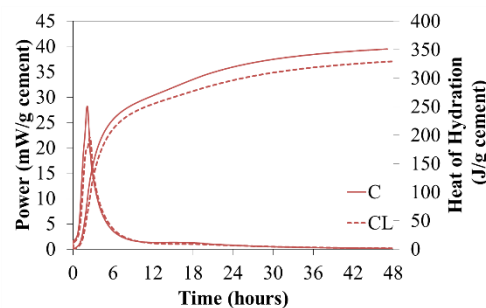
(d) Plant C at 140 °F

Figure 4.3. Isothermal Calorimetry of cements from plants A and C at 73°F and 140°F.

Isothermal calorimetry was also performed on cement pastes from plant A and plant C at 140°F with the following supplementary cementitious materials (SCMs): 50% slag and 15% fly ash (Class C and Class F). Pastes were prepared at a w/c = 0.44, which is the maximum w/c specified for class AAA concrete in GDOT Section 500.

Figure 4.4 shows the isothermal calorimetry heat evolution curves of cements from plants A and C with SCMs. For the finer Type IL cement (AL), Type IL cement showed an accelerated hydration reaction with all SCMs when compared to the companion Type I/II cement with SCMs, as indicated by the left shift of the heat release (power) curves. Additionally, the peaks of power evolution were higher for Type IL cements when compared to their companion Type I/II cements. This results in faster hydration kinetics, which may result in greater early strength. On the other hand, the coarser Type IL cement (CL) showed slower hydration with all SCMs with lower peaks of power evolution when compared to the companion Type I/II cement with SCMs. This indicates slower hydration reaction kinetics and therefore suggest slower early strength gain.

(a) Plant A   (b) Plant C
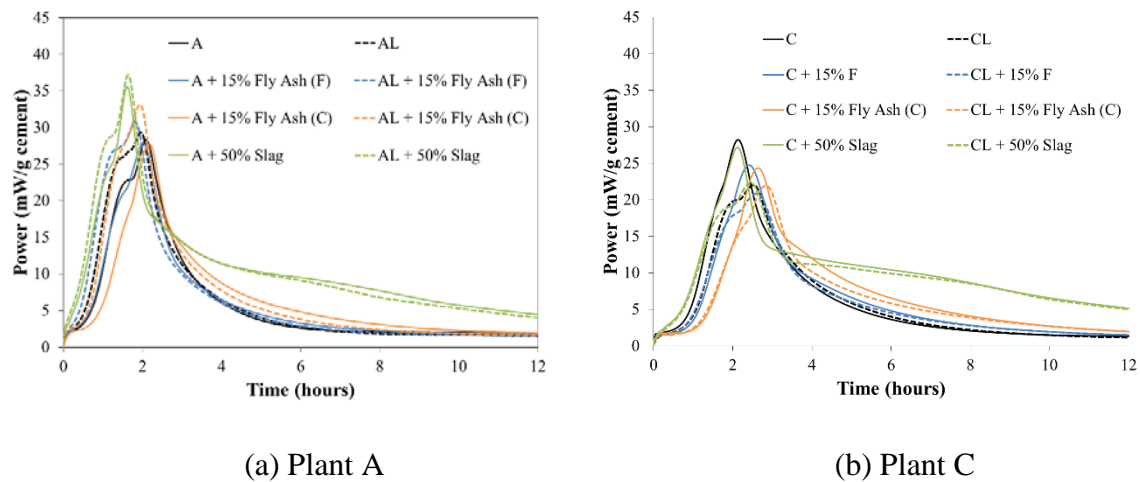
Figure 4.4. Isothermal calorimetry heat evolution curves for cements from plants A and C with supplementary cementitious materials (SCMs).

Figure 4.5 shows the cumulative heat of hydration curves for cements from plants A and C with SCMs. For the finer Type IL cement (AL), Type IL cement with SCMs showed similar cumulative heat of hydration to the companion Type I/II cement with SCMs. This may indicate similar quantity of hydration microstructure, which may result in equivalent strength values on the long term. On the other hand, the coarser Type IL cement (CL) showed ~5% lower cumulative heat of hydration with all SCMs than Type I/II cement. This may indicate that lower quantity of hydration microstructure, which may result in lower strength values in the long term.
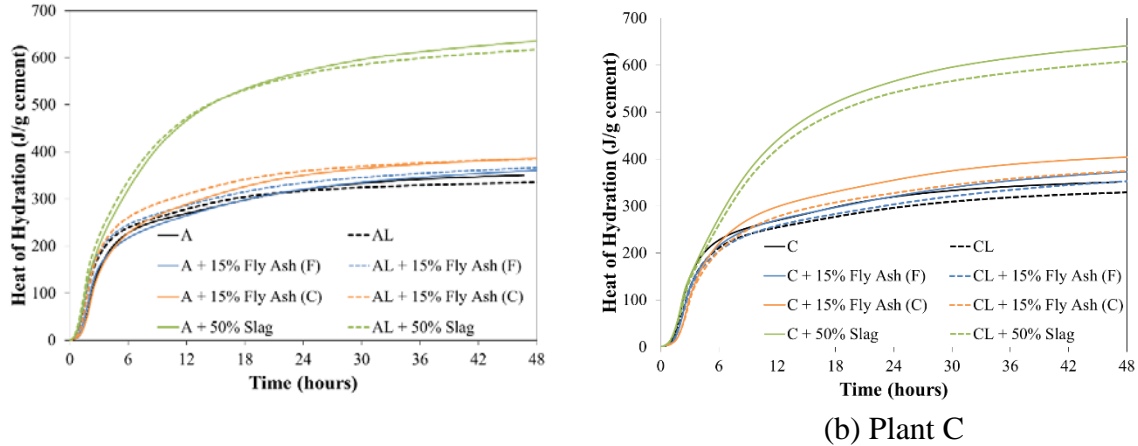
(a) Plant A

(b) Plant C

Figure 4.5.   Cumulative heat of hydration (power) curves for cements from plants A and C with supplementary cementitious materials (SCMs).

4.1.3 Quantitative X-ray diffraction analysis (QXRD)

Table 4.2 shows the results of the QXRD analysis for Type I/II and Type IL cements from plants A – E. The chemical compositions of all Type I/II cements followed the specifications of ASTM C 150. Plant E had the highest amount of C_3S, which contributed to early age microstructural and strength development. Plants A and B had more C_2S, which contributed to later microstructural and strength development. Plant D had the highest percentage of C_3A and Plant B had the most C_4AF.

4.1.4   Time of setting

Vicat time of setting testing was performed on cement pastes at 73°F and at 140°F for the Cements A-E. Pastes were prepared at a w/c = 0.31, which was previously determined to be the normal consistency of Cement B and which produced similar quality pastes for the other cements. The same w/c was used for all cements and blended cements.

As shown in Figure 4.6, Vicat tests demonstrated that limestone cements generally set faster than Type I/II cements. Cement CL was the only limestone cement that had similar setting time when compared to Type I/II cements at 73°F.

At 140°F, and comparing the initial set of Type IL cements to their companion Type I/II cements, Type IL cements experienced slightly earlier initial set. Regarding the final set, the general trend was that Type IL cements tended to experience final set earlier, except for Cement C, where they set at almost the same time. When comparing among Type IL cements of the same source but with different finenesses (Cement E), the finer cements experienced earlier initial set but similar final set. However, the differences between the Type I/II and IL cement setting times were much smaller at 140°F than at 73°F. Practically, they are so similar that variations may not be noticed at this higher temperature.

44

Table 4.2. QXRD analysis results

Phase Name	Cement Source										
	A	AL	B	BL	C	CL	D	DL	E	EL C	EL F
C_3S	52.10	50.83	55.85	54.26	60.89	52.74	55.49	53.51	64.29	61.86	54.39
C_2S	24.15	17.31	21.62	15.30	16.39	17.88	17.42	15.32	13.14	7.58	14.65
C_3A cubic	2.95	3.27	2.78	2.10	1.90	1.54	4.22	4.10	4.23	3.83	3.30
C_3A orthorhombic	0.01	0.00	0.19	0.49	0.00	0.00	0.73	0.55	0.00	0.07	0.14
C_3A TOTAL	2.96	3.27	2.97	2.59	1.90	1.54	4.95	4.65	4.23	3.90	3.44
C_4AF	10.31	9.28	12.85	13.53	12.16	12.09	10.83	9.88	10.55	10.31	10.30
Lime	0.26	0.10	0.34	0.16	0.25	0.19	0.42	0.27	0.28	0.04	0.00
Periclase	3.11	2.23	0.19	0.26	0.81	0.48	0.33	0.14	0.98	1.39	1.73
Quartz	0.03	0.10	0.07	0.32	0.23	0.30	0.45	0.83	0.06	0.18	0.31
Arcanite	0.26	1.09	0.32	1.26	0.01	0.15	0.29	0.41	1.10	1.76	2.16
Gypsum	0.25	0.75	0.00	0.01	0.01	0.01	0.01	0.01	0.03	0.02	0.10
Bassanite / PLASTER	1.99	1.60	3.19	3.32	2.45	2.99	3.86	2.94	1.62	1.05	0.28
Anhydrite	0.06	0.12	1.55	0.87	0.06	0.01	0.07	0.04	0.17	2.34	1.77
Calcite	3.24	12.15	1.07	7.90	4.22	10.82	4.15	10.47	2.39	8.28	9.78
Portlandite	1.29	1.18	0.00	0.21	0.63	0.82	1.74	1.52	1.17	1.32	1.12

(a) 73°F   (b) 140°F
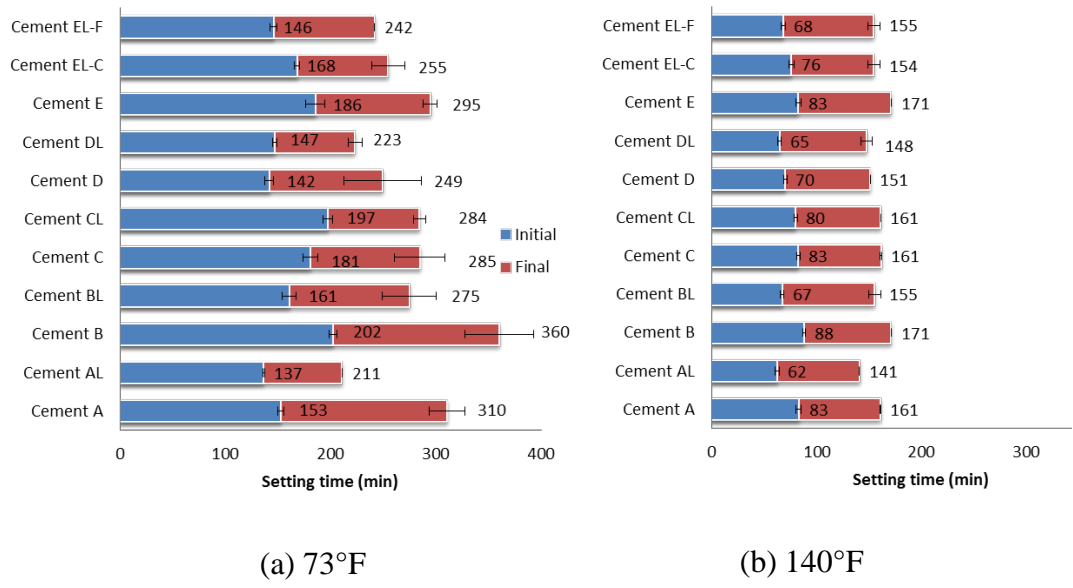
Figure 4.6. Time of setting of cements "A" to "E" at 73°F and 140°F.

4.2 Fresh Concrete Properties

Slump, unit weight, and air content of fresh class AAA concrete were measured for all mixes that used the mix design given in Table 3.2 and using a w/c of 0.32. Figure 4.7 shows the slump, unit weight, and air content results, respectively. Type IL cement showed lower slump values for both sources. The unit weight was similar for all cements. The air content was slightly higher for non-air entrained concretes using Type IL cement when compared to Type I/II cement, and the difference was more significant for cement CL.

4.3 Mechanical Properties

4.3.1 Compressive strength development

Compressive strength of concrete [ASTM C39] cylinders was measured for class AAA concrete at 0.25 day, 0.75 day, 1 day, 3 days, 7 days, 28 days, 56 days, and 90 days.

Figures 4.8 and 4.9 show the concrete compressive strength results of class AAA concrete from plant A and plant C, respectively. The results in Figure 4.8 (Cement A/AL) showed that cement AL (Type IL) resulted in higher (~200%) 1-day compressive strength than cement A (Type I/II). At 90 days, the difference in strength decreased where AL showed ~6% higher values. Cement AL had the finer particle size distribution than cement A. The results in Figure 4.9 (Cement C/CL) showed that cement CL (Type IL) resulted in relatively lower compressive strength than cement C (Type I/II) at all

46

ages. At 90 days, compressive strength with cement C was about 5% higher than with cement CL. Cement C and CL had similar particle size distribution.
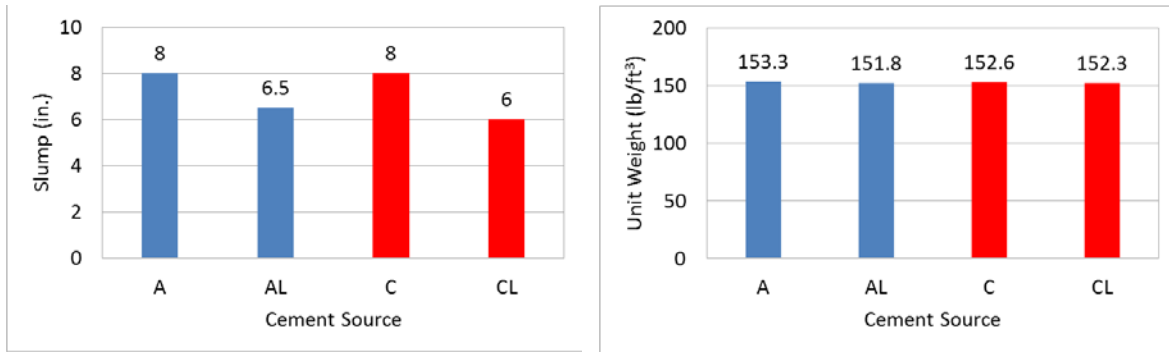
(a) Slump

(b) Unit weight
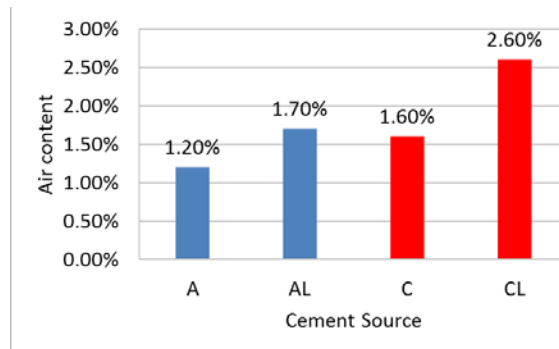
(c) Air content

Figure 4.7. Fresh properties of class AAA concrete with Type I/II and Type IL cements from sources A and C.
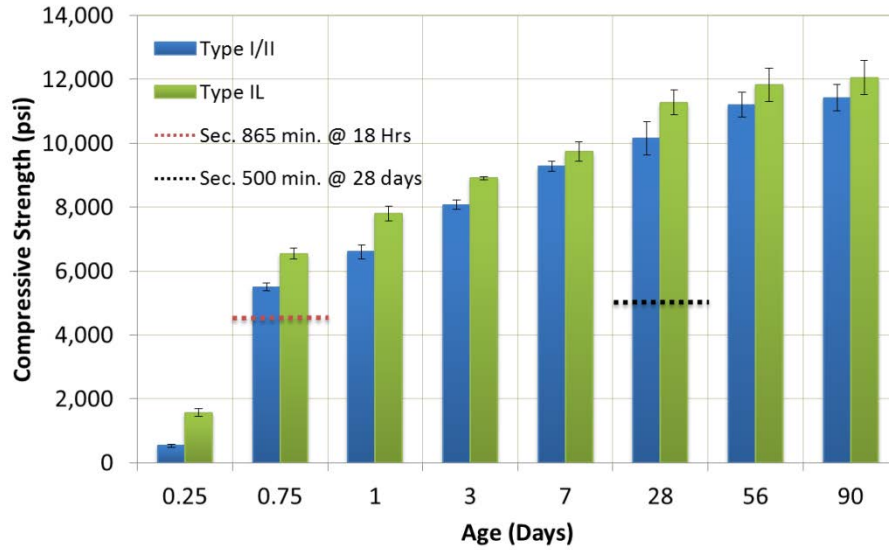
Figure 4.8. Compressive strength of class AAA concrete from plant A. The GDOT specified strengths for class AAA concrete are shown as dotted lines for 0.75 and 28 days.
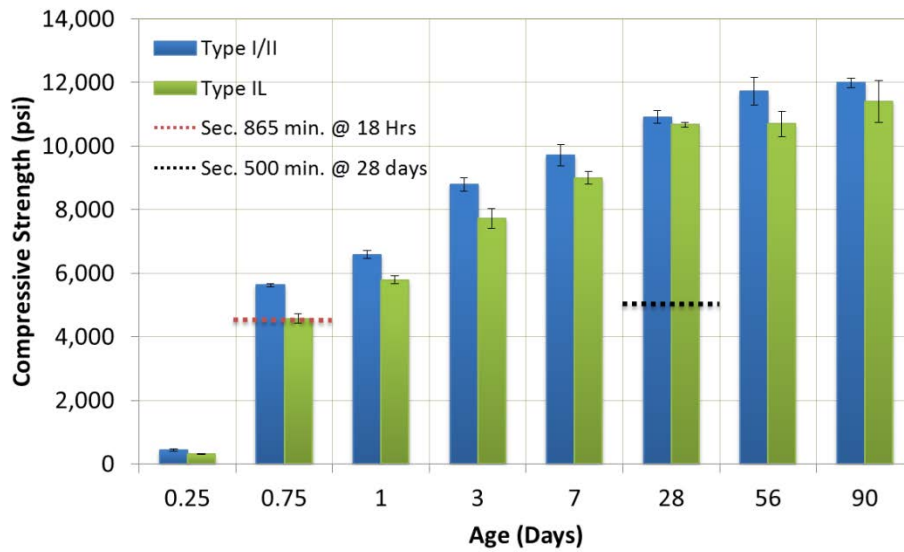
Figure 4.9. Compressive strength of class AAA concrete from plant C. The GDOT specified strengths for class AAA concrete are shown as dotted lines for 0.75 and 28 days.

In addition to room temperature curing (at 73°F) described above, and as mentioned earlier; a high-temperature curing regime was also used for a second group of concrete

mixes produced using cements C and CL. To simulate possible precast operations, concrete was cured at 140°F for the first 18 hours, followed by curing at room temperature (73°F). According to GDOT Specification 865 [2013], the minimum required strength for stress release of prestressed concrete I-beams is 4500 psi at 18 hours of age. In addition, GDOT Specification 500 [2013] specifies the minimum compressive strength at 28 days for class AAA concrete to be 5000 psi.

Figure 4.10 shows the compressive strength of concrete made with cement from plant C for Type I/II and Type IL, and cured at 73°F and 140°F. For concrete cured at both temperatures, cement C (Type I/II) showed about 10% higher 1-day compressive strength than concrete made with cement CL (Type IL). Also, the compressive strength of the concrete with accelerated thermal-curing showed about 30% higher strength at 18 hours. At 56 days, the strength of the concrete cured at room temperature (73°F) was higher than the strength of thermally-cured concrete by about 5% to 10%.

The compressive strength of all the concrete mixes was higher than the minimum requirements of GDOT Specifications 865 and 500.
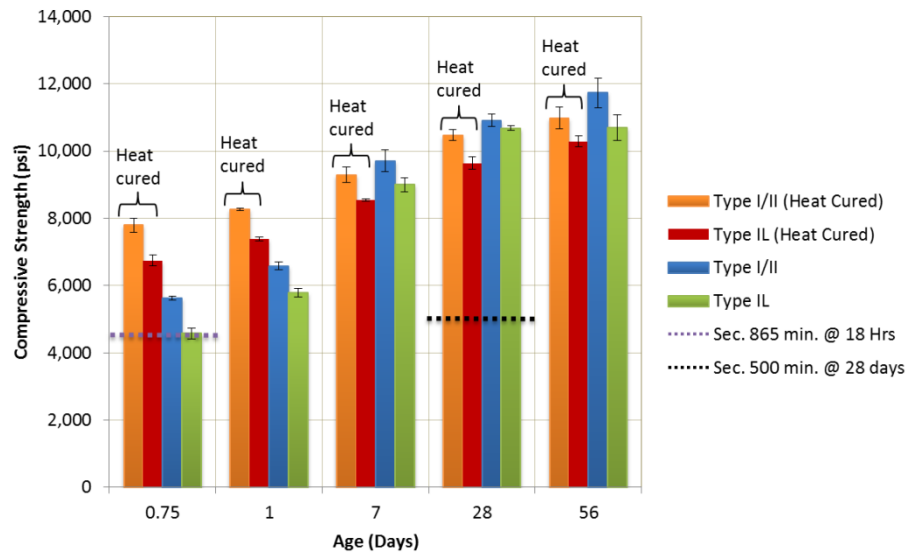
Figure 4.10. Compressive strength of class AAA concrete from plant C cured at 73°F and heat cured at 140°F.

4.3.2 Elastic modulus [ASTM C469]

Elastic modulus was measured for concrete samples at 28 days of age.   Figure 4.11 shows the elastic modulus [ASTM C469] for class AAA concrete made with cements A, AL, C and CL measured at 28 days. The elastic modulus of cement A and AL were similar, while cement C had a slightly higher elastic modulus than cement CL (~5%).
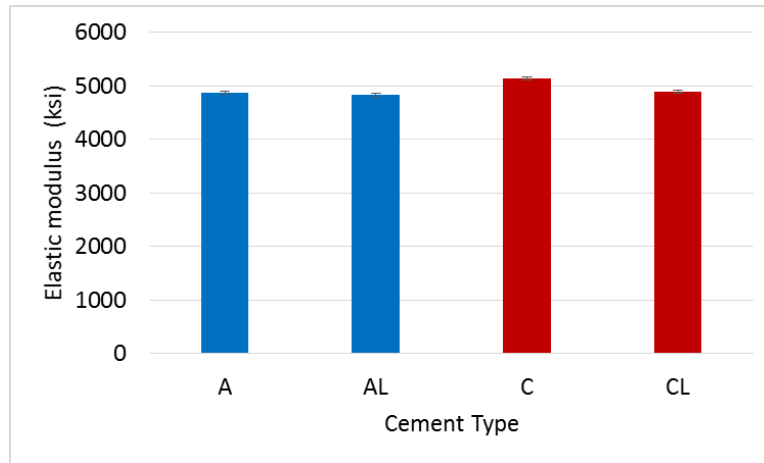
Figure 4.11. Elastic modulus values of Type I/II and Type IL cements from plants A and C (class AAA concrete)

4.3.3 Splitting tensile strength [ASTM C496, AASHTO T 198]

Splitting tensile strength was measured for concrete samples at 28 days of age. No significant differences were observed between Type I/II and Type IL cements as shown in Figure 4.12.
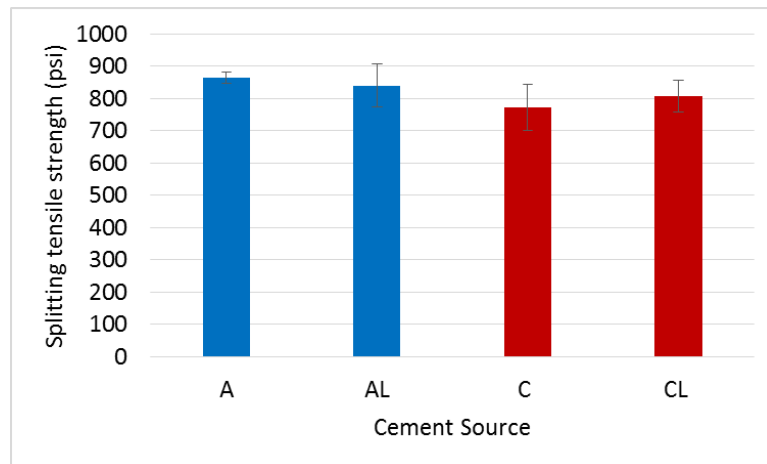
Figure 4.12. Splitting tensile strength of Type I/II and Type IL cements from plants A and C (class AAA concrete)

4.4 Shrinkage, Creep, and Permeability

4.4.1 Drying shrinkage

Drying shrinkage prisms [ASTM C157] were lime-water bath cured for 28 days, and then drying initiated and was measured at 4 days, 7, days, 14 days, 4 weeks, 8 weeks, 16 weeks, and 32 weeks. Another group of samples was only cured for 7 days, and then drying was measured at the same drying times mentioned before [Alabama DOT Standard Specifications for highway construction Section 501]. In general, the results show that finer limestone cements had similar shrinkage values to Type I/II cements while coarser limestone cements had lower shrinkage values than Type I/II cement. The results also showed that shorter period of curing leads to higher drying shrinkage.

Drying shrinkage was measured for class AAA concrete mixes made with Type I/II and Type IL cements from plant A and plant C. Samples were cured for 28 days in a saturated lime-water bath [ASTM C157]. After that, the concrete prisms were taken out to dry at 73°F.

Figure 4.13 shows the drying shrinkage results for Type I/II and Type IL cements from plant A (Cement A and AL) and plant C (cement C and CL) cured at 73°F for class AAA concrete. Shrinkage values for class AA concrete are shown for comparison. The strain values were computed based on the length of the prism measured immediately after being removed from the lime-water bath.

For class AAA concrete, cement AL showed lower drying shrinkage than cement A (~10% at 112 days). On the other hand, for class AA concrete, cement AL showed higher drying shrinkage values than cement A at all ages (~20% at 112 days). The greater shrinkage of the class AA concrete is likely related to the higher w/c, despite its lower cement content compared to AAA concrete. The w/c of class AAA was 0.320 while that of class AA was 0.445.

For plant A, class AAA concrete showed lower drying shrinkage than class AA concrete by 112 days. The difference was more significant for Type IL where cement AL from class AAA showed about 30% lower shrinkage than cement AL for class AA, whereas cement A from class AAA showed only 5% lower shrinkage than cement A from class AA concrete.

For cements C and CL of class AAA concrete, cement C showed higher drying shrinkage than cement CL (~10% at 112 days). For cement C, class AAA concrete showed ~10% lower drying shrinkage than class AA concrete by 112 days, while CL AAA concrete showed ~20% lower shrinkage than class AA concrete by 112 days.
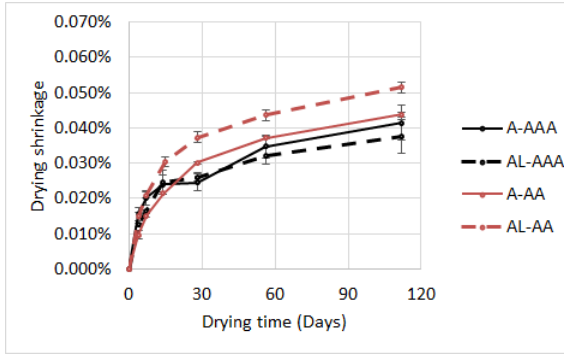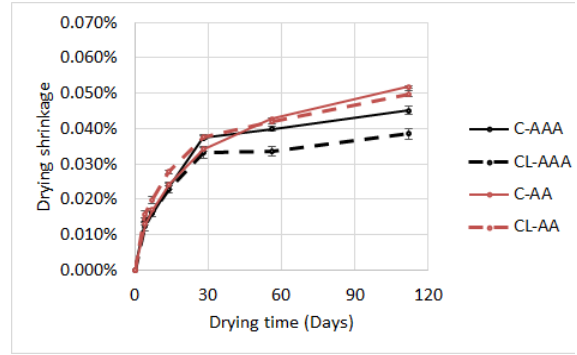
3. (a) Cement A/AL   4. (b) Cement C/CL

Figure 4.13. Drying shrinkage [ASTM C157] of Type I/II and Type IL cements
from plants A and C with class AAA and class AA concrete.

A second group of class AAA concrete prisms was cured for only 7 days in a
saturated lime-water bath to show the effect of curing time on drying shrinkage. After
curing, the concrete prisms were taken out to dry at 73°F. Figure 4.14 shows the drying
shrinkage results for concretes made with cement A/AL and C/CL and cured at 73°F for
7 days as well as those cured for 28 days. For cements A and AL, the samples cured for
7 days showed higher drying shrinkage than samples cured for 28 days (~40% for Type
I/II and ~45% for Type IL at 112 days). The drying shrinkage values of A and AL cured
for 7 days differed by less than 5%.

For cements C and CL, the samples cured for 7 days showed higher drying shrinkage
than samples cured for 28 days (~25% for Type I/II and ~50% for Type IL at 112 days).
The drying shrinkage values of C and CL cured for 7 days differed by less than 4%.
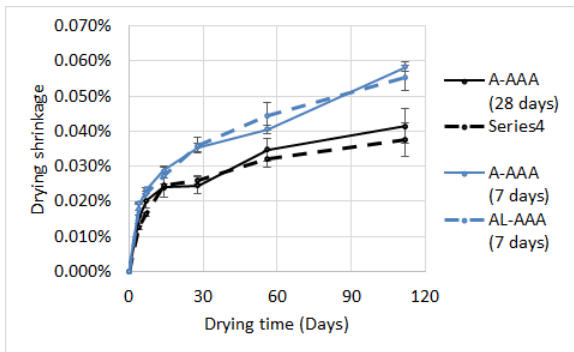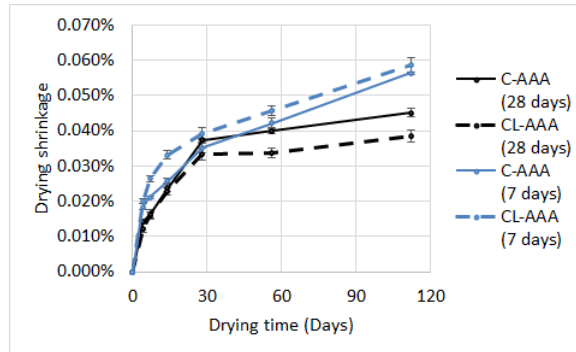
(a) Cement A/AL   (b) Cement C/CL

Figure 4.14. Drying shrinkage of Type I/II and Type IL cements from plants A and
C cured for 7 days and 28 days.

4.4.2 Creep [ASTM C512]

Creep samples were cured for 3 days and then loaded at age of 3 days at 40% of their compressive strength capacity. Loading at 3 days of age was selected to simulate the age at which cutting of the prestressing strands was performed for the four prestressed beams.

Creep tests were initialized for class AAA concrete for Type I/II and Type IL cements from plant A (cement A and cement AL) and plant C (cement C and CL). The 4-in. diameter x 15-in. long cylinder samples were cured in a lime-water bath at room temperature. The total combined creep plus shrinkage strain was measured for 5000 hours. Shrinkage strain was measured on unloaded cylinders subjected to identical temperature and humidity conditions. This shrinkage strain was subtracted from the total strain to give the creep strain. That creep strain was divided by the unit stress, often termed specific creep. The specific creep results are shown in Figure 4.15.

Specific creep of A and AL showed relatively similar values up to 1500 hours. However, at about 5000 hours, the creep of A was about 10% higher than that of AL.

Specific creep of C and CL initially showed relatively close values. However, at about 200 hours their creep rates changed and by about 5000 hours, the specific creep values for C (Type I/II) were about 40% greater than those of CL (Type IL).
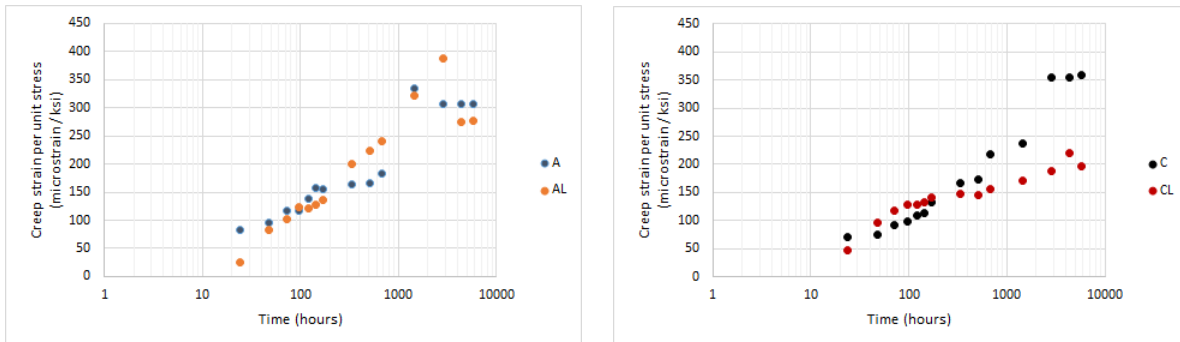
(a) Cement A/AL   (b) Cement C/CL

Figure 4.15. Specific creep of Type I/II and Type IL cements from plant A and C.

4.4.3 Permeability

Permeability of the class AAA, class AA, and class A concretes was determined by testing surface resistivity [AASHTO TP 95, 2011] and the ability to Resist Chloride Ion Penetration (RCPT) [AASHTO T 277, 2011, and ASTM C 1202, 2012].

Surface resistivity (SR) was measured for the class AAA and class AA concrete mixtures using the procedures outlined in AASHTO TP 95-11. (This 2011 provisional standard has recently been adopted as a full standard under the designation AASHTO T 358-15. Surface preparation of test specimens differs between AASHTO T 358 and TP 95-11 specifications, but all equipment and measurements are otherwise unchanged.) Measurements were recorded after 1, 3, 7, 14, 28, 56, 90, and 180 days of hydration and a plot of SR development over time was created for each mixture (Figure 4.16).
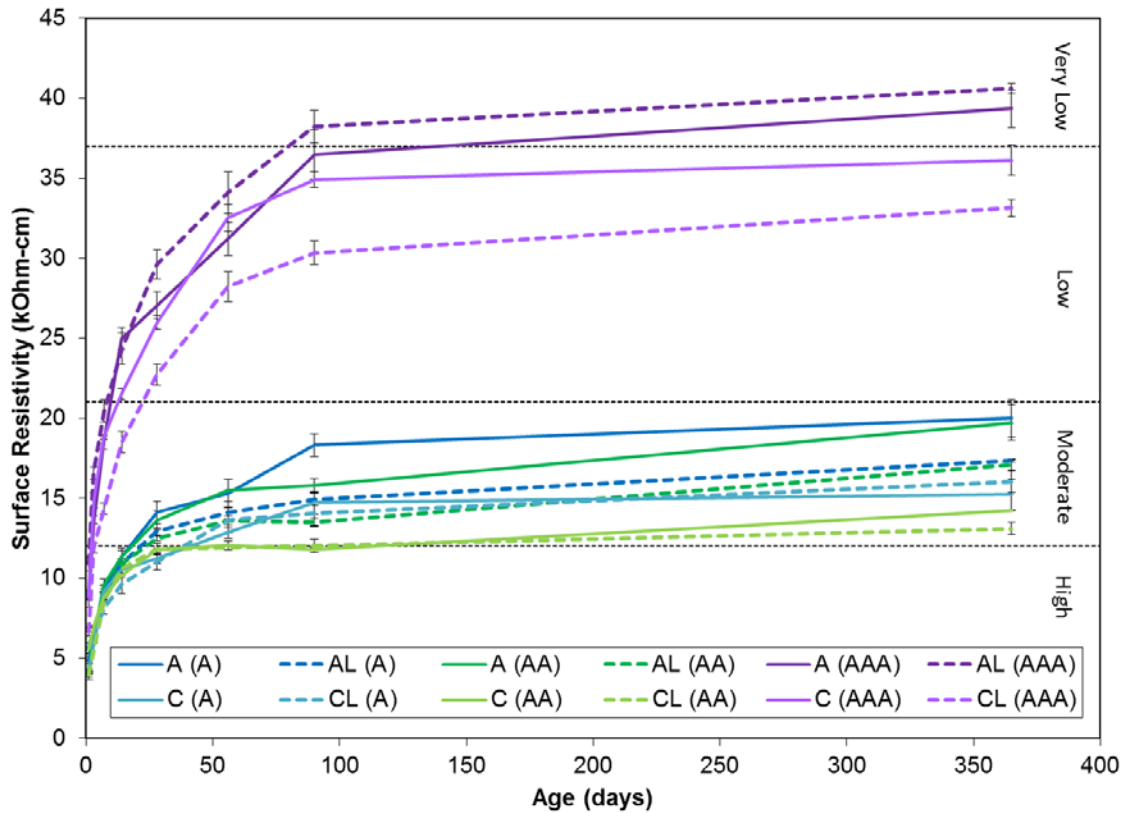
Figure 4.16. Surface resistivity for class AAA concretes made with A, AL, C and CL cements.

The class AAA concrete mixtures overall measured greater surface resistivity values at all ages compared to the class AA control mixtures. By 28 days, the class AAA mixtures were found to have a "low" permeability classification by AASHTO TP 95, while the class AA mixtures were found to have "high" to "moderate" permeability classifications. These designations were consistent with those measured by the ASTM C1202/AASHTO T277 rapid chloride permeability test (RCPT), performed after 56 days of hydration, although the SR test showed greater differences between mixtures than the RCP test did. The observed reduction in permeability is likely due to the lower water-to-

cement ratio (w/c) of the class AAA mixtures, which is known to reduce porosity and pore interconnectivity, especially at w/c below about 0.41 [Mehta and Monteiro, 2006].

Comparing cement types, the class AAA mixtures containing Type I/II and Type IL cements each exhibited different rates of SR development, but yielded similar RCPT results at 56 days (Figure 4.17). Mixture AL-AAA showed the greatest increase in SR over time, and by 90 days exceeded the 37 kOhm-cm threshold for "very low" permeability. On average, it exhibited SR values 5-10% greater than its companion mixture made from Cement A. Mixture CL-AAA showed the least increase in SR over time, but still achieved "low" permeability classification by 28 days. On average, it exhibited SR values 10-15% lower than that of its companion mixture made from Cement C. These differences in SR development between the Type I/II and Type IL mixtures are consistent with the differences in strength development previously noted, which suggests that the nucleation and filler effects observed for finely ground Type IL cements (e.g., Cement AL) produce concrete with a more refined microstructure and consequently with higher strength and lower permeability [Sun et al. 2013, and Kadri et al. 2010]. On the other hand, Type IL cements ground to similar fineness as traditional portland cements (e.g., Cement CL) tend to have behavior more dominated by dilution effects, which result in the formation of less hydration product and consequently lower strength and higher permeability [Bentz et al. 2009; Bonavetti et al. 2003; and Barcelo et al. 2013].
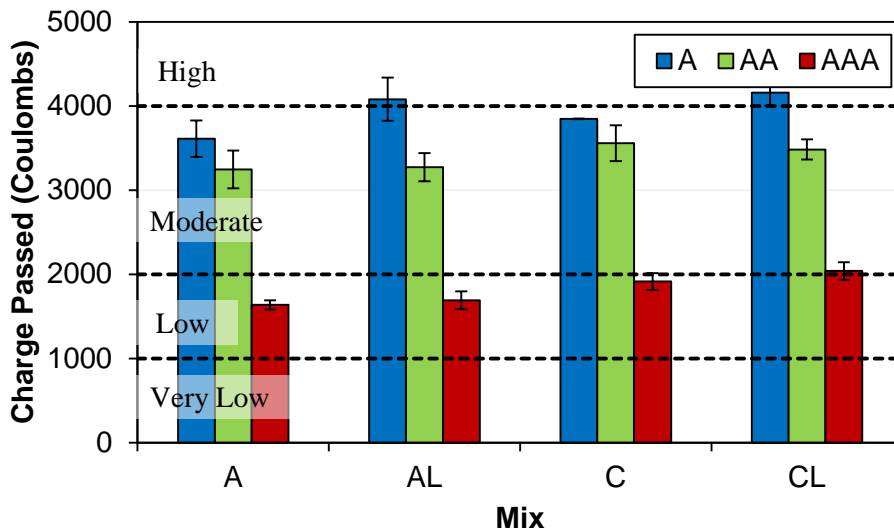

Figure 4.17. Chloride ion permeability (RCPT) for class A, AA, and AAA concretes at 56 days.

The RCPT results show that the permeability of the class AAA concrete made with Type IL cements as well as the Type I/II cements satisfies GDOT Specification 500 [2013] with the special provision requirements for high performance concrete (HPC) for

bridge girders and that the cement AL and the A and C cements satisfy the HPC pile requirements. Concrete with CL cement was within 2% of satisfying HPC pile requirements (2040 Ω vs 2000 Ω required, within error of the experiment).

4.5 Prestressed Concrete Beam Performance

As discussed in Sections 3.8 through 3.10, four 10-in. wide by 25-in deep by 30-ft. long beams were constructed, two with class AAA concrete C and two with class AAA concrete CL delivered to the precast concrete plant via ready-mix trucks. The beams were reinforced with two ½-in. diameter grade 270 low relaxation prestressing strands, each initially jacked to about 31 kips (204 ksi). These beams together with concrete samples were used to determine prestressing losses, influence of cement type on strand bond, strand transfer length, strand development length, and flexural capacity. The principal objective was determining the comparative behavior of beams made with Type I/II and Type IL cements.

4.5.1 Prestress losses

Prestress loses were measured using vibrating wire gages that were placed at midspan of each beam at the level of the prestressing strands. When comparing the strain values with respect to readings measured immediately before strand release, the strain from combined elastic, creep and shrinkage showed that strains in beams made with CL had averaged about 2% less strain than those made with C; that is, there was practically no difference in total strain.

Figure 4.18 shows the change in concrete strain at mid-span of each prestressed beam relative to the strain values measured before strand-release. The prestressing strands were released 3 days after placing the concrete. Compression due to strand release caused the immediate measured strain values to increase (elastic losses). The measured strain values continued to increase for the following 3 months due to drying shrinkage and creep.

Figure 4.19 shows a comparison of the total prestressing losses of the beams compared to the value calculated using AASHTO LRFD [2016] "refined" prestressing losses equations. The average total prestress loss for beams made with Type IL were about 5% lower than the values calculated using AASHTO equations, while the average total losses for beams made with Type I/II were about 6% less than the calculated values.
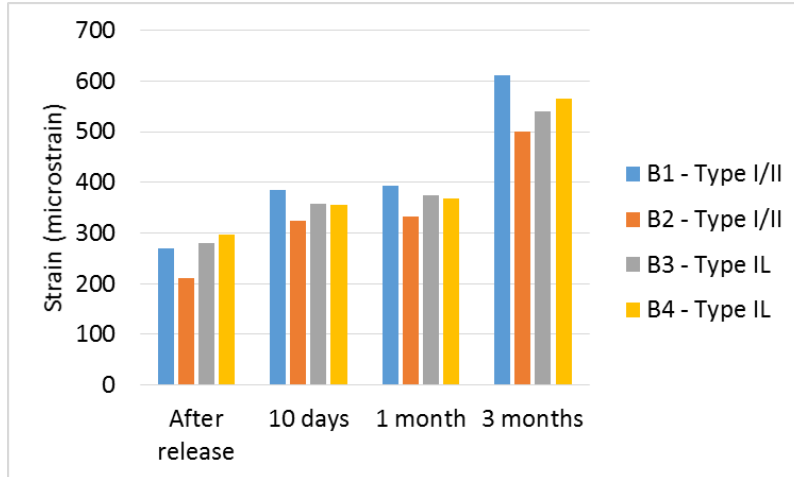
Figure 4.18. Strain values of prestressed beams at level of strands with respect to values taken before release.
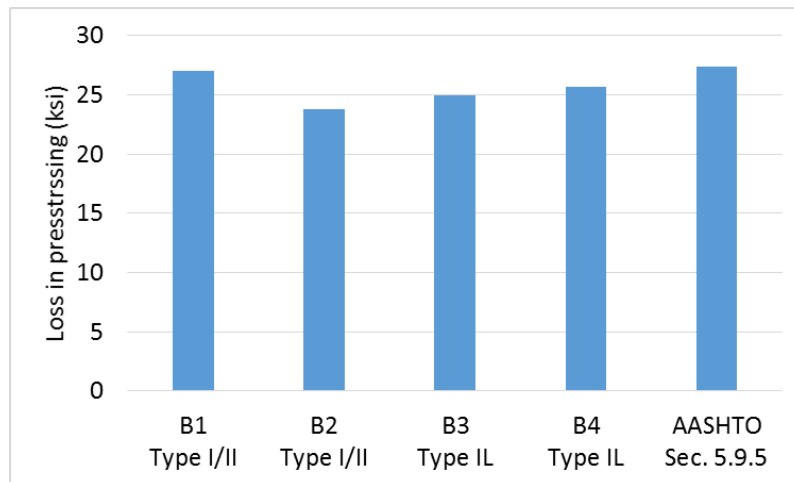
Figure 4.19. Total prestress losses in comparison to AASHTO LRFD [2016] calculations.

When comparing the ratio of the change in strain with respect to the strain values after release, Type IL cement showed lower values than Type I/II cement as shown in Figure 4.20. This implied that beams with Type IL cement underwent lower combined creep and drying shrinkage than beams with Type I/II cement.

Overall, the prestress losses found in pretensioned beams made with Type I/II cement and with Type IL cement were similar and were less than total losses specified in AASHTO LRFD [2016] using the refined method.
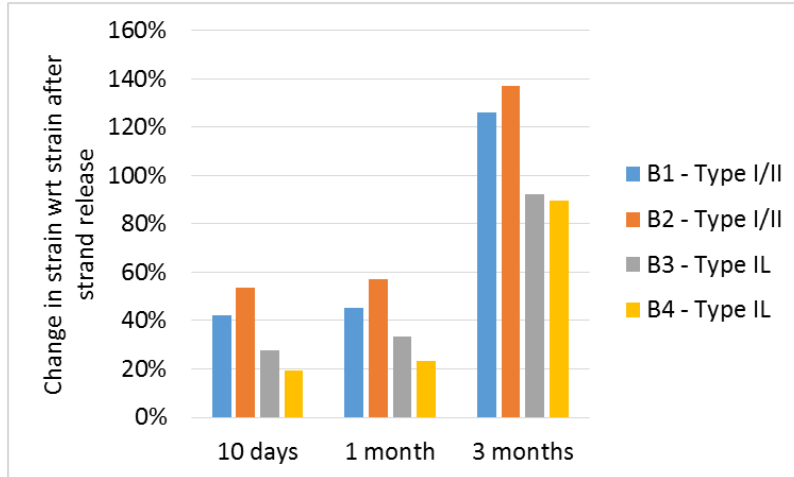
Figure 4.20. Prestress losses with respect to strain values after release.

4.5.2 Strand Bond using Mustafa test for direct pull-out

Mustafa test for direct pull-out was performed to compare the direct bond strength of prestressing strands with concretes made with Type I/II and Type IL cements. The results showed that limestone cement performed similarly to Type I/II cement.

The tests were performed on the samples that were prepared using the same concrete used for placing the precast prestressed beams. Two 2-ft x 2-ft x 3-ft long concrete blocks were prepared with six prestressing strands in each block. One block was made with Type I/II cement while the other was made with Type IL cement. Each of the six ½-in. diameter strands in each block was pulled out with a center-hole hydraulic jack. The strands were pulled until yielding with no observed slip. One of the wires in a strand in the Type IL sample broke after yielding, and no slip occurred in that case as well.

The results showed similar behavior between strands embedded in concretes with Type I/II and Type IL cements as illustrated by the load-displacement plots in Figure 4.21.   These Mustafa tests indicated that the strand-concrete bond was the same for concretes made with Type I/II and with Type IL cements.

58
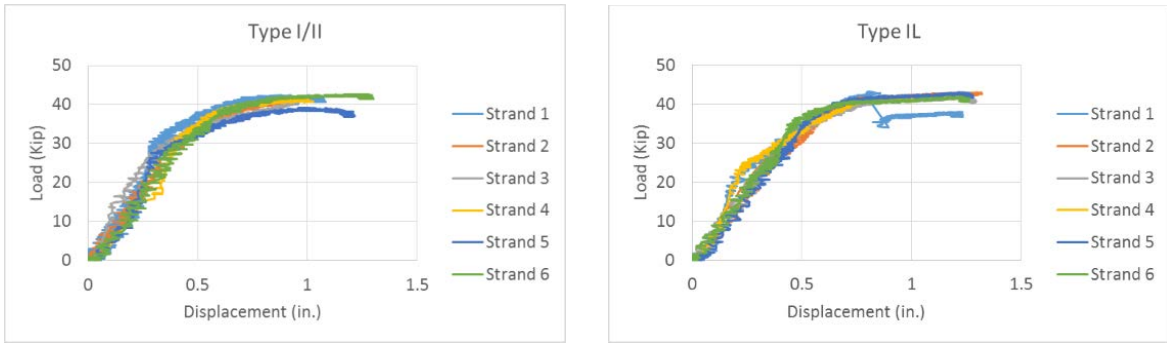
Figure 4.21. Mustafa pull-out test results.

4.5.3 Transfer length

The results of the transfer length measurements are given in Figures 4.22 through 4.25 for beams 1 through 4, jacking (right in figure) and dead (left in figure) ends, respectively.
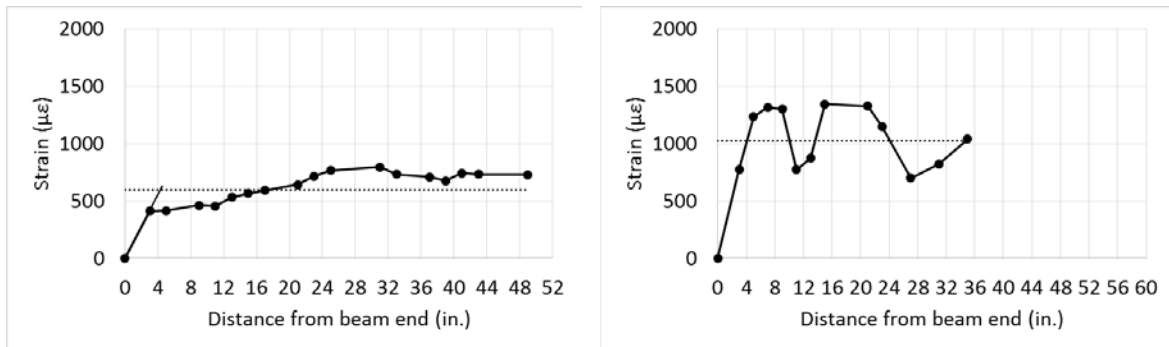
Figure 4.22. Beam 1 (Type I/II) concrete surface strain measurements for transfer length
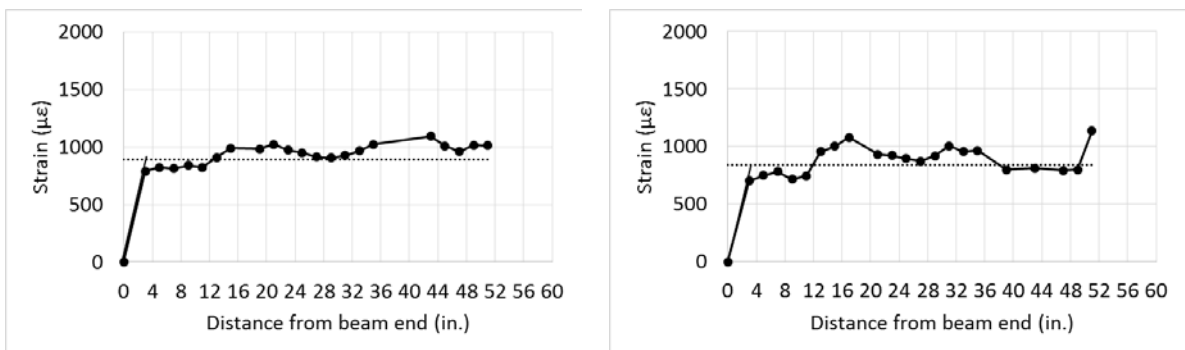
Figure 4.23. Beam 2 (Type I/II) concrete surface strain measurements for transfer length

59
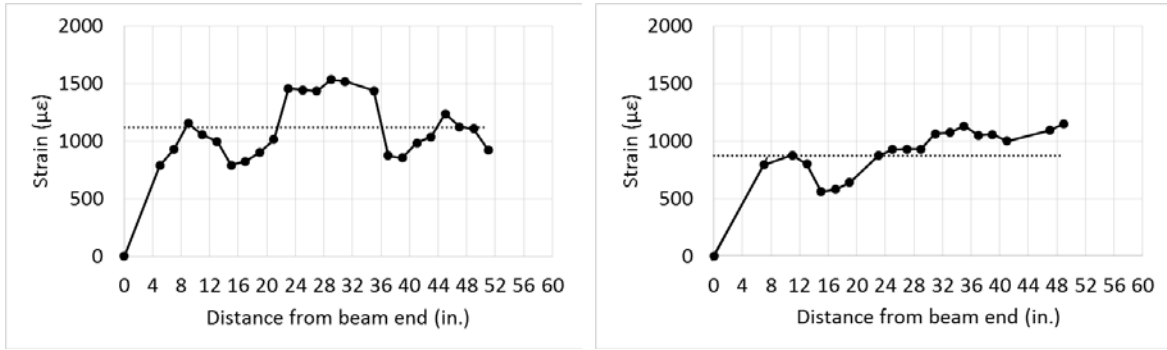
Figure 4.24. Beam 3 (Type IL) concrete surface strain measurements for transfer length
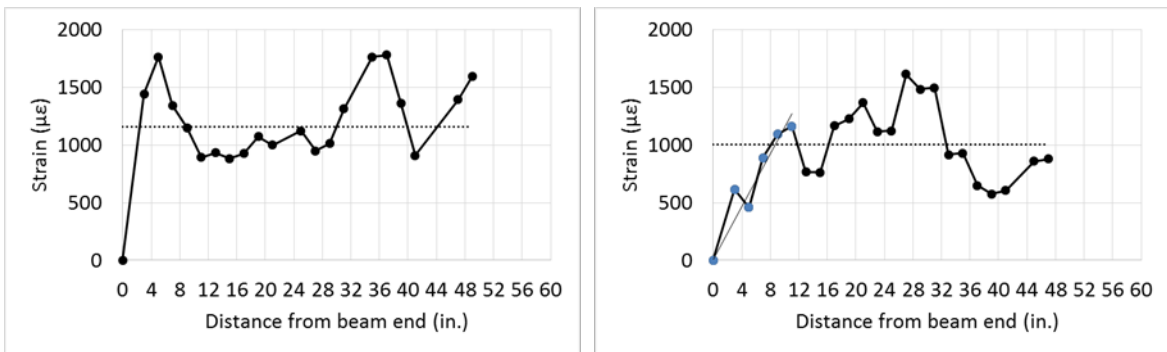
Figure 4.25. Beam 4 (Type IL) concrete surface strain measurements for transfer length

The transfer length measurements at the dead (anchor) end of Beam 1 were considered poor because of the poor consolidation of the first batch of concrete used in this location; the DEMEC points came loose. Therefore, transfer length data from beam 1 are suspect. The other data are consistent; although there is a large variation in the "constant strain" region due to poor bond of the DEMEC points and the concrete.

Nevertheless, by use of the technique developed by Russell [1992], the data were averaged and the transfer length was determined as the intersection of the initial slope of the strain and 95% of the mean strain where the strain is constant. Table 4.3 presents the resulting development lengths. The experimental results were compared with those specified by AASHTO LRFD [2016] and by ACI 318-14 [2014]. The AASHTO value is determined as 60 d_b where d_b is the strand diameter. The ACI value is equal to $(f_{se}/3000)$x d_b where f_{se} is the effective stress in the prestressing strands after losses. The f_{se} value was determined using the measured initial and final stress in the strands by the embedded vibrating wire strain gages.

Table 4.3 Summary of transfer lengths of beams 1 to 4

Cement Type	Beam number	End type	Transfer length (in)	Average (in.)	AASHTO LRFD 5.11.4.2 (in.)	ACI 318 (in.)	Measured / AASHTO
I/II	1	Jacking	4	4	30	29.5	13%
I/II	1	Dead	4				
I/II	2	Jacking	4	4	30	30.0	13%
I/II	2	Dead	4				
IL	3	Jacking	8	8	30	29.8	27%
IL	3	Dead	8				
IL	4	Jacking	3	6	30	29.7	20%
IL	4	Dead	9				

The results show that transfer lengths were less than 30% of the AASHTO LRFD [2016] specified length for the beams made using Type IL cement.

4.5.4 Development length

As described in chapter 3, loads were applied at various distances from the end of the beam based on theoretical [AASHTO LRFD, 2016] development length (L_d) values. The ratio of the end distances ranged from 90% of L_d to 45% of L_d. The results showed no strand slip in any of the beams. Two development length tests were performed on each beam by applying a concentrated load at a specific distance from one of the supports.

The first test applied the concentrated load at 90% of L_d. If no strand slip was measured, the second test applied the concentrated load at 65% of L_d. If no strand slip was measured, the third test applied the concentrated load at 50% of L_d. Finally, if no strand slip was measured in the third test, the forth test applied the concentrated load at 45% of L_d.

The first beam from each cement type was used for the 90% L_d and 65% L_d tests, while the second beam was used for the 50% L_d and 45% L_d tests. The concentrated load was applied at one end for the 90% L_d test while the concentrated load was applied at the opposite end of the beam for the 65% L_d test to avoid loading cracked areas of the beam. Similarly, the concentrated load was applied at one end for the 50% L_d test while the concentrated load was applied at the opposite end of the beam for the 45% L_d.

Figure 4.26 shows a schematic diagram showing the points of application of the concentered load for the first test.
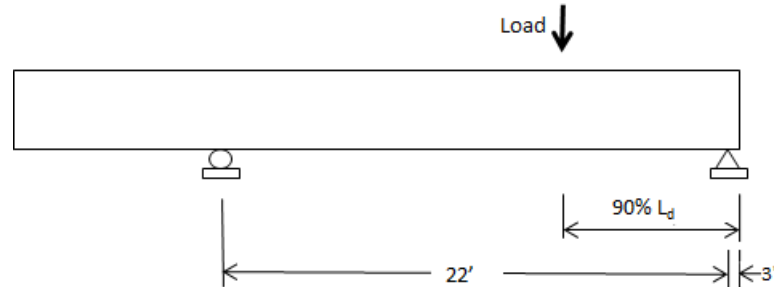
Figure 4.26. Schematic diagram for the first beam test.

Figure 4.27 shows the load-deflection curves collected from the eight development length tests. The results show similar behavior for beams made with Type I/II and Type IL cements. There was no strand slip observed at any of the tests, implying that the development length was less than 45% of the value calculated using the AASHTO LRFD (2016) equations. It should be noted that for the last test of the beam with Type I/II cement, the beam was intentionally loaded until the section collapsed.

Overall, the strand development length in beams made of Type I/II and Type IL cement was the same and satisfied AASHTO LRFD Bridge Design Specifications.
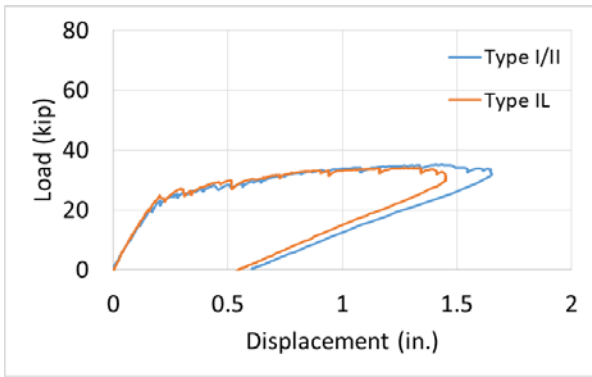
(a) Load applied at 90% of L_d (b) Load applied at 65% of L_d
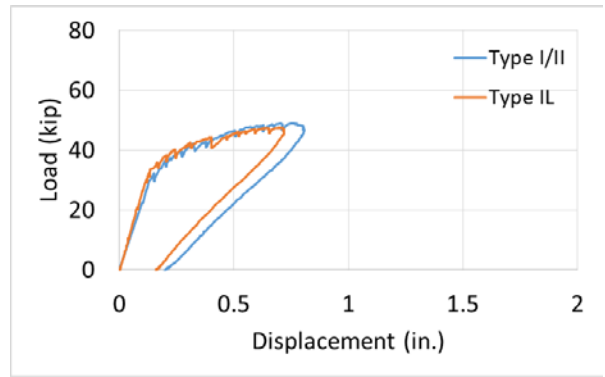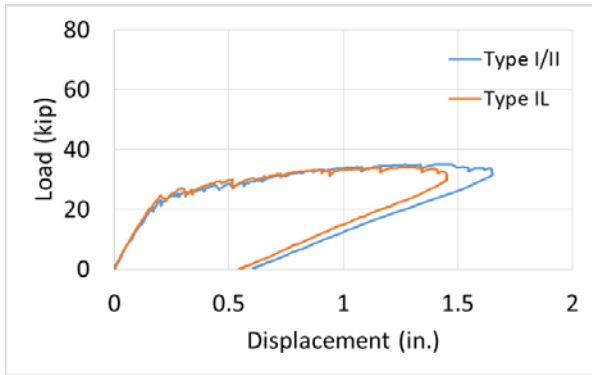
(c) Load applied at 50% of L_d (d) Load applied at 45% of L_d
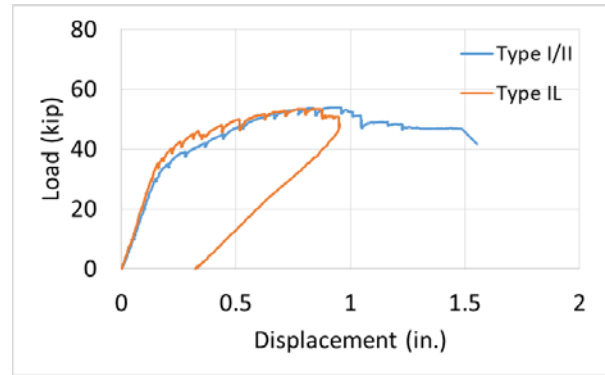
Figure 4.27. Load-deflection values of the development length tests.

4.5.5 Flexural Capacity

As described in Chapter 3, the load was applied at midspan during the third test of each beam to compare the flexural capacities of the beams and those capacities with calculated values. The experimental load-displacement results are shown in Figure 4.28; beams made with Type I/II and those with Type IL cements behaved the same. Beam 1 (B1) was not tested in flexure because there was a large unconsolidated pour joint at the midspan due to the delay in delivery of the ready-mix Type I/II concrete.
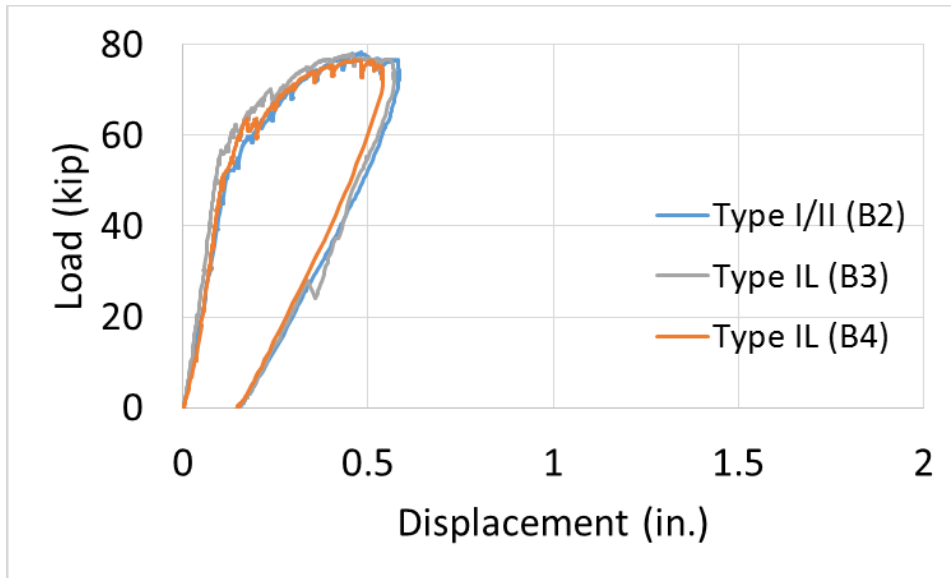
Figure 4.28. Load-displacement results of the flexure test of Beams 2 through 4.

The nominal flexural moment capacity of each beam was calculated based on Equation 5.7.3.2.2-1 of AASHTO LRFD [2016] and was compared to the value determined from the flexural tests. For both the beams made from the Type I/II and Type IL cements, the average experimental moment capacity was 5% greater than the calculated nominal moment capacity. The AASHTO procedure gave conservative results for the beams made with Type IL cement.

Chapter 5 – Conclusions and Recommendations

This research examined the use of portland limestone cement (Type IL) with up to 15% replacement of portland cement with interground limestone in high-early strength concrete for prestressed concrete bridge applications. Cement suppliers in the Southeast supplied portland cement of traditional composition (i.e., meeting the current AASHTO M 85 specifications for high early strength) and a companion limestone blended cement, produced from the same clinker but with nominally, 15% by mass, interground limestone to meet AASHTO M 240 [2012] specifications. Concrete mixes were developed that satisfied the performance requirements of Georgia Department of Transportation (GDOT) Standard Specifications Section 500 [2013] for class AAA structural concrete.

Conventional portland cements Type I/II and portland limestone cements Type IL from five manufacturers were characterized. Cements from two manufacturers designated as A and C were investigated in detail for high early strength concretes for use in transportation structures like bridge girders. Cements were A and AL (manufacturer A Type I/II and Type IL, respectively), plus C and CL (manufacturer C Type I/II and Type IL, respectively). Concretes with supplementary cementitious materials included class F fly ash at 15% replacement, class C fly ash at 15 % replacement, and ground granulated blast furnace slag at 50% replacement.

The following conclusions were made based on this research.

5.1 Material Characteristics

The fineness of the cement and of the limestone particles affected the hydration kinetics, which in turn affected key properties such as strength gain and dimensional stability. The fineness of the portland cement from the manufacturers was similar but the fineness of the interground limestone was finer or of the same fineness as the portland cement. Pastes and concretes made with Type IL cements with finer ground limestone showed faster hydration compared to those with Type I/II cements. The finer material led to faster setting time and higher compressive strength. Pastes and concretes with coarser ground limestone showed similar setting time but lower compressive strength than those made with Type I/II cements and concretes with finer ground limestone. At higher temperatures, however, the Type I/II and IL cements showed quite similar setting times, suggesting that in precast concrete applications the effect of cement fineness is less significant.

5.2 Material Properties

Concretes with a design strength of 8000 psi were made with Type IL cement and with water-to-cementitious ratio (*w/cm*) of 0.32 and were used to achieve higher early strength ranging from 4600 psi to 6500 psi when cured at 73°F for 18 hours for cements from plant C and plant A, respectively. Under the same 73°F lime-water bath curing for 28 days, the compression strengths ranged from 10500 to 11100 psi for cements from plant C and plant A, respectively. These strengths satisfy Georgia Specification section 865 [2013] class AAA concrete for use in precast prestressed concrete girders.

Class AAA concrete made using Type IL cements from plant C were heat cured at 140°F and had an 18-hour strength of 6700 psi. The heat-cured strength of the companion concrete made with Type I/II cement was 15% greater than that with Type IL cement. Heat curing did not appear to negatively affect longer term performance of the concrete.

Elastic modulus and splitting tensile strength of concretes made with Type I/II and Type IL cements (both fine and coarse ground) were statistically similar.

Permeability of the high early strength concrete made with Type IL and Type I/II cements (GDOT class AAA) as measured by surface resistivity [AASHTO TP 95, 2011] and by RCPT [AASHTO T 277, 2011] was low. At 56 days, the RCPT test showed that concretes made with Type IL cement gave chloride ion permeability of 1690 coulombs and 2040 coulombs for concretes made with cements AL and CL, respectively. An RCPT of 2000 coulombs or less is considered high performance concrete in Georgia Specification section 500 [2013].

5.3 Structural Performance

Two 30-ft long precast pretensioned concrete beams were made using Type IL cement from plant C and two were made using Type I/II cement from plant C. Both were reinforced with ½-in. diameter grade 270 low relaxation prestressing strand and were stressed identically. Tests examined strand bond, prestress losses, transfer and development length of the strand, and flexural strength. The following conclusions were made based on the performance of these prestressed concrete beams.

The bond capacity of the ½-in. strand found using Mustafa direct pull-out test [Logan, 1997] showed no difference in performance between Type IL and Type I/II cement. No strand slip was observed in any of the pull-out tests; yielding was developed in all strands.

The average total prestress losses (decrease in force in the prestressing strands) found in beams made with Type IL cement was about 2% less than the average total loss found in beams made with Type I/II cement – essentially no difference. These losses were about 5% less than those predicted using the "refined method" given in the AASHTO LRFD Bridge Design Specifications [2016].

Transfer length of the ½-in. strands in the beams made with Type IL cement was less than 30% of the transfer length specified in AASHTO LRFD [2016]. Development length of those strands was less than 45% of the development length specified in AASHTO LRFD [2016].

The flexural moment capacity of the prestressed concrete beams was about 5% greater than the nominal moment capacity calculated based on AASHTO LRFD [2016]. AASHTO specifications provide a conservative flexural capacity for precast prestressed beams made using Type IL cements satisfying AASHTO M 240 [2012] specifications.

5.4 Recommendations

Overall, this research on Type IL cements for high early strength concretes demonstrated that Type IL cements satisfying AASHTO M 240 [2012] specifications may be used in place of Type I/II cements which satisfy AASHTO M 85 [2012] specifications for construction of transportation structures such as precast prestressed bridge girders.

Therefore, on a preliminary basis, it is recommended that Type IL cements, which satisfy AASHTO M 240 [2012] specifications, may be used in place of Type I/II cements for high early strength concrete for transportation structures such as precast prestressed concrete beams.

It is recommended that that the Georgia DOT Standard Specifications Section 830.2.01 (Portland or Blended (Hydraulic) Cement) and Section 865.2.01 (Prestressed Concrete Bridge Members) be amended to permit the use of Type IL cements. Appendix A gives such specific recommendations.

References

AASHTO LRFD (2016), *AASHTO LRFD Bridge Design Specifications (7th Edition),* with 2015 and 2016 Interim Revisions, American Association of State Highway and Transportation Officials, Washington, DC

AASHTO M 240 (2012) "Standard Specification for Blended Hydraulic Cements American Association of State Highway and Transportation Officials, Washington, DC.

AASHTO M 85 (2012), "Standard Specification for Portland Cement", American Association of State Highway and Transportation Officials, Washington, DC

AASHTO T 277 (2011), "Standard Method of Test for Electrical Indication of Concrete's Ability to Resist Chloride Ion Penetration", American Association of State Highway and Transportation Officials, Washington, DC

AASHTO T 358 (2015), "Standard Method of Test for Surface Resistivity Indication of Concrete's Ability to Resist Chloride Ion Penetration." American Association of State Highway and Transportation Officials, Washington, DC.

AASHTO TP 95 Provisional Standard (2011), "Standard Method of Test for Surface Resistivity Indication of Concrete's Ability to Resist Chloride Ion Penetration." American Association of State Highway and Transportation Officials, Washington, DC.

Alabama DOT Standard Specifications for Highway Construction (2012), Section 501, Structural Portland Cement Concrete, Montgomery, Alabama 36130, pp. 727

ASTM C 114 (2013), "Standard Test Methods for Chemical Analysis of Hydraulic Cement", ASTM International, West Conshohocken, PA, DOI: 10.1520/C0114-13

ASTM C 1202 (2012), "Standard Test Method for Electrical Indication of Concrete's Ability to Resist Chloride Ion Penetration", ASTM International, West Conshohocken, PA, 10.1520/C1202-12

ASTM C 1365 (2011), "Standard Test Method for Determination of the Proportion of Phases in Portland Cement and Portland-Cement Clinker using X-Ray Powder Diffraction Analysis", ASTM International, West Conshohocken, PA, 10.1520/C1365-06R11

ASTM C 138 (2014) "Standard Test Method for Density (Unit Weight), Yield, and Air Content (Gravimetric) of Concrete," ASTM International, West Conshohocken, PA

ASTM C 143 (2016), "Standard Test Method for Slump of Hydraulic-Cement Concrete," ASTM International, West Conshohocken, PA,

ASTM C 150 (2016), "Standard Specification for Portland Cement", ASTM International, West Conshohocken, PA, 10.1520/C0150-16

ASTM C 150, (2004) "Standard Specification for Portland Cement", ASTM International, West Conshohocken, PA, 10.1520/C0150-04

ASTM C 157 (2014), "Standard Test Method for Length Change of Hardened Hydraulic-Cement Mortar and Concrete," ASTM International, West Conshohocken, PA

ASTM C 1608 (2012), "Standard Test Method for Chemical Shrinkage of Hydraulic Cement Paste", ASTM International, West Conshohocken, PA, 10.1520/C1608-12

ASTM C 1698 (2009), "Standard Test Method for Autogenous Strain of Cement Paste and Mortar", ASTM International, West Conshohocken, PA, 10.1520/C1698-09

ASTM C 191 (2013), "Standard Test Methods for Time of Setting of Hydraulic Cement by Vicat Needle", ASTM International, West Conshohocken, PA, 10.1520/C0191-13

ASTM C 192 (2016), "Standard Practice for Making and Curing Concrete Test Specimens in the Laboratory", ASTM International, West Conshohocken, PA, 10.1520/C0192_C0192M-16

ASTM C 204 (2011), "Standard Test Methods for Fineness of Hydraulic Cement by Air-Permeability Apparatus", ASTM International, West Conshohocken, PA, 10.1520/C0204-11E01

ASTM C 231 (2014), "Standard Test Method for Air Content of Freshly Mixed Concrete by the Pressure Method," ASTM International, West Conshohocken, PA

ASTM C 39 (2016), "Standard Test Method for Compressive Strength of Cylindrical Concrete Specimens", ASTM International, West Conshohocken, PA, 10.1520/C0039_C0039M-16

ASTM C 469 (2002). "Standard Test Method for Static Modulus of Elasticity and Poisson's Ratio of Concrete in Compression," American Society for Testing and Materials, West Conshohocken, PA, pp. 5

ASTM C 496 (2011), "Standard Test Method for Splitting Tensile Strength of Cylindrical Concrete Specimens", ASTM International, West Conshohocken, PA, 10.1520/C0496_C0496M-11

ASTM C 512 (2015), "Standard Test Method for Creep of Concrete in Compression," ASTM International, West Conshohocken, PA

ASTM C 595, (2012) "Standard Specification for Blended Hydraulic Cements", ASTM International, West Conshohocken, PA, 10.1520/C0595-12E01

ASTM C 618 (2015), "Standard Specification for Coal Fly Ash and Raw or Calcined Natural Pozzolan for Use in Concrete", ASTM International, West Conshohocken, PA, 10.1520/C0618-15

ASTM E 1131 (2008). "Standard Test Method for Compositional Analysis by Thermogravimetry," American Society for Testing and Materials, West Conshohocken, PA, pp. 5

Balonis, M. and F.P. Glasser, (2009). The density of cement phases. Cement and Concrete Research, 39(9): p. 733-739.

Barcelo, L., M.D.A. Thomas, K. Cail, A. Delagrave, and B. Blair (2013), "Portland Limestone Cement Equivalent Strength Explained," Concrete International, 35(11), p. 41-47

Barcelo, L., M.D.A. Thomas, K. Cail, A. Delagrave, and B. Blair, (2013). Portland Limestone Cement Equivalent Strength Explained. Concrete International, 35(11): p. 41-47

Bentz, D.P. ; T. Sato, I. de la Varga, and W.J. Weiss (2012) "Fine limestone additions to regulate setting time in high volume fly ash mixtures," Cement and Concrete Composites, V34:11-17.

Bentz, D.P., E.F. Irassar, B.E. Bucher, and W.J. Weiss (2009), "Limestone Fillers Conserve Cement; Part 2: Durability issues and the effects of limestone fineness on mixtures," Concrete International, 31(12), p. 35-39

Bonavetti, V., H. Donza, G. Menendez, O. Cabrera, and E.F. Irassar (2003), Limestone filler cement in low w/c concrete: A rational use of energy. Cement and Concrete Research, 33(6): p. 865-871.

Bonavetti, V.; H. Donza, V. Rahhai, and E. Irassar (2000) "Influence of initial curing on the properties of concrete containing limestone blended cement", Cement and Concrete Research, V.30:703-8.

De Weerdt, K., K.O. Kjellsen, E. Sellevold, and H. Justnes, (2011b). Synergy between fly ash and limestone powder in ternary cements. Cement & Concrete Composites,. 33(1): p. 30-38

De Weerdt, K., M. Ben Haha, G. Le Saout, K.O. Kjellsen, H. Justnes, and B. Lothenbach, (2011a). Hydration mechanisms of ternary Portland cements containing limestone powder and fly ash. Cement and Concrete Research, 41(3): p. 279-291

GDOT Specification 500, (2013) *Georgia Department of Transportation (GDOT), Standard Specifications for Construction of Transportation Systems, Section 500 - Concrete Structures.* Georgia Department of Transportation, Atlanta, Georgia

GDOT Specification 865, (2013) *Georgia Department of Transportation (GDOT), Standard Specifications for Construction of Transportation Systems, Section 865 Manufacture of Prestressed Concrete Bridge Members*, Georgia Department of Transportation, Atlanta, Georgia

Hawkins, Peter; Tennis, Paul D.; and Detwiler, Rachel J.; (2003) The Use of Limestone in Portland Cement: A State-of the-Art Review, EB227, Portland Cement Association, Skokie, Illinois, USA, 44 pages.

Holland, R.B; R. Moser, L. Kahn, P. Singh, and K. Kurtis (2012), *Durability of Precast Prestressed Concrete Piles in Marine Environments, Part 2: Concrete,* (FHWA-GA-12-1026) Final Report, GDOT Research Project No. 10-26 Task Order No. 02-78, Georgia Department of Transportation, Atlanta, Georgia

Isaia, G.C., A.L.G. Gastaldini, and R. Moraes, (2003), Physical and pozzolanic action of mineral additions on the mechanical strength of high-performance concrete. Cement & Concrete Composites, 25(1): p. 69-76

Kadri, E.H., S. Aggoun, G. De Schutter, and K. Ezziane, (2010). Combined effect of chemical nature and fineness of mineral powders on Portland cement hydration. Materials and Structures, 43(5): p. 665-673.

Kahn, L. et al. (2005), "High Strength/High Performance Concrete for Precast Prestressed Bridge Girders in Georgia," Final Report, Research Project No. 9510, Office of Materials and Research, Georgia Department of Transportation, pp. 173.

Livesey, P., (1991) "Strength characteristics of Portland-limestone cements," Construction and Building Materials, 5(3): p. 147-150.

Logan, D. R. (1997), "Acceptance Criteria for Bond Quality of Strand for Pretensioned Prestressed Concrete Applications," PCI Journal, March/April 1997, pp. 52-90.

Lothenbach, B., G. Le Saout, E. Gallucci, and K. Scrivener, (2008), Influence of limestone on the hydration of Portland cements. Cement and Concrete Research, 38(6): p. 848-860.

Lothenbach, B.; G. Le Saout, E. Gallucci, and K. Scrivener (2008) "Influence of limestone on the hydration of Portland cements", Cement and Concrete Research, V.38:848-60.

Matschei, T., B. Lothenbach, and F.P. Glasser, (2007), The role of calcium carbonate in cement hydration. Cement and Concrete Research, 37(4): p. 551-558.

Mehta, P.K. and P.J.M. Monteiro (2006), *Concrete: microstructure, properties, and materials*, 3rd ed., McGraw-Hill, New York, pp. 659

Menendez, G., V. Bonavetti, and E.F. Irassar, (2003). Strength development of ternary blended cement with limestone filler and blast-furnace slag. Cement & Concrete Composites, 25(1): p. 61-67

Nadelman, Elizabeth, (2016), *Hydration and Microstructural Development of Portland Limestone Cement-Based Materials*, Ph.D. Dissertation, Georgia Institute of Technology, Atlanta, Georgia

Oey, T., A. Kumar, J.W. Bullard, N. Neithalath, and G. Sant, (2013). The Filler Effect: The Influence of Filler Content and Surface Area on Cementitious Reaction Rates. Journal of the American Ceramic Society, 96(6): p. 1978-1990.

Russell, B.W. (1992). Design Guidelines for Transfer, Development and Debonding of Large Diameter Seven Wire Strands in Pretensioned Concrete Girders. Doctoral Thesis, The University of Texas at Austin

Sun, H.F., B. Hohl, Y.Z. Cao, C. Handwerker, T.S. Rushing, T.K. Cummins, and J. Weiss, (2013); "Jet mill grinding of portland cement, limestone, and fly ash: Impact on particle size, hydration rate, and strength", Cement & Concrete Composites, 44: p. 41-49

Tennis, P.D., M.D.A. Thomas, and W.J. Weiss, (2011), *State-of-the-art report on use of limestone in cements at levels of up to 15%*. Portland Cement Association, SN3148, Skokie, Illinois, p. 78.

Vance, K., M. Aguayo, T. Oey, G. Sant, and N. Neithalath, (2013). Hydration and strength development in ternary portland cement blends containing limestone and fly ash or metakaolin. Cement & Concrete Composites, 39: p. 93-103

Appendix A – Preliminary Recommendations for Revision of Georgia DOT Standard Specifications

A.1 Revision to Section 830.2

Based upon research presented in this report and concurrent research sponsored by the Georgia Department of Transportation, the following revision to Section 830.2 is proposed where revised content is shown in red:

830.2.01 Portland or Blended (Hydraulic) Cement

A. Requirements

Use only hydraulic cements that are listed in QPL 3.

1. Types

Use **portland or blended** cement that meets the requirements in AASHTO M85 or M240. Hydraulic cement types include:

Use	High Early Strength Concrete	Remaining Portland Cement Concrete
M85 Portland cement	Types I or III	Types I or II
M240 Blended cement	**Type IL**	**Type IL**

2. Ensure that the Portland cement concrete meets the low alkali and the false set requirements of AASHTO M85.

3. Do not use cement that is damaged, partially set, lumpy, or caked.

4. Mixing and Storing: Do not mix or store different brands or types of cement in the same bin. Do not mix or store the same brand of cement from different mills in the same bin.

B. Fabrication

General Provisions 101 through 150.

C. Acceptance

See the requirements in AASHTO M 85 or AASHTO M 240.

A.2 Revision to Sections 865.1 and 865.2

Based upon research presented in this report and concurrent research sponsored by the Georgia Department of Transportation, the following revisions to Sections 865.1 and 865.2 are proposed where revised content is shown in red:

865.1.01 Related References

B. Referenced Documents

AASHTO M 55

AASHTO M 85

AASHTO M 221

AASHTO M 240

AASHTO T 22

AASHTO T 27

ASTM A 123/A 123M) ASTM A 153/A 153M)

ASTM A 185

ASTM A 416

ASTM A 497

AASHTO Specification for Highway Bridges

Laboratory SOP-3, Standard Operating Procedures for Precast/Prestressed Concrete

QPL 9

GDT 35

865.2.01 Prestressed Concrete Bridge Members

A. Requirements

1. Portland Cement

Use Type I, Type II, or Type III cement that meets requirements of AASHTO M 85 **or Type IL that meets requirements of AASHTO 240 for low alkali cement**.

a. Use Type II cement in concrete to cast pile for specific locations noted on the Plans.